



TEKSTİL VE MÜHENDİS
(Journal of Textiles and Engineer)



<http://www.tekstilvemuhendis.org.tr>

Empirical Equations and Poisson's Ratios for Initial Load-Extension Properties of Some Complex Glass and Aramid Technical Weft Knitted Structures

Bazı Karmaşık Cam ve Aramid Teknik Atkı Örme Kumaşların Başlangıç Yük-Uzama Özellikleri için Ampirik Denklemler ve Poisson Oranları

Arif KURBAK¹, Sinem ÖZTÜRK²

¹Dokuz Eylül University, Textile Engineering Department, Izmir, Turkey

²SUN Tekstil Research and Development Center, Torbalı, Izmir, Turkey

Online Erişime Açıldığı Tarih (Available online):31 Aralık 2019 (31 December 2019)

Bu makaleye atıf yapmak için (To cite this article):

Arif KURBAK, Sinem ÖZTÜRK (2019). Empirical Equations and Poisson's Ratios for Initial Load-Extension Properties of Some Complex Glass and Aramid Technical Weft Knitted Structures, Tekstil ve Mühendis, 26: 116, 381-405.

For online version of the article: <https://doi.org/10.7216/1300759920192611611>

Sorumlu Yazara ait Orcid Numarası (Corresponding Author's Orcid Number) :

<https://orcid.org/0000-0002-5391-3335>

EMPIRICAL EQUATIONS AND POISSON'S RATIOS FOR INITIAL LOAD-EXTENSION PROPERTIES OF SOME COMPLEX GLASS AND ARAMID TECHNICAL WEFT KNITTED STRUCTURES

Arif KURBAK^{1*}

<https://orcid.org/0000-0002-5391-3335>

Sinem ÖZTÜRK²

^{1*}Dokuz Eylül University, Textile Engineering Department, Izmir, Turkey

²SUN Tekstil Research and Development Center, Torbalı, Izmir, Turkey

Gönderilme Tarihi / Received: 25.04.2019

Kabul Tarihi / Accepted: 02.12.2019

ABSTRACT: This work builds on former research carried out concerning load-extension properties of plain knitted glass technical fabrics. In related former research, it was determined that a load-extension or a load-contraction curve could be considered in three stages of extension or contraction. These stages were a) the extension or contraction of the fabric (the first stage), b) the extension of the yarn along with the change of the shape of the sample (the second stage), and, c) the extension or contraction of the fibres (the third stage). In the same works, theoretical analyses were then provided to explain the first stage of extension or contraction, and thus some simple equations between load and extension and between load and contraction together with Poisson's ratio were obtained. In obtaining the extension of the loop head curve, the equation of extension of a circular ring had been applied. This formulation enabled the emergence of a method that separates the frictional restrains and/or fabric jamming forces from the experimentally obtained quadratic curve fittings for plain knitted fabrics. Building on those former studies, for the present work, similar experimental studies for the first stages of extensions or contractions, were carried out for some more complex technical weft knitted structures that use E-glass and Aramid yarns. The curve fitting equations are obtained and some empirical equations are given, assuming that the same method of separating frictional restrains and/or fabric jamming forces from quadratic curve fittings also applies for complex structures. Extension and contraction rates are also calculated and discussed further. These empirical equations can, of course, be used in related engineering software.

Keywords: Weft knitted fabric, load-extension, contraction, empirical equations, glass fiber, aramid fiber, initial extension rates, initial contraction rates.

BAZI KARMAŞIK CAM VE ARAMİD TEKNİK ATKI ÖRME KUMAŞLARIN BAŞLANGIÇ YÜK-UZAMA ÖZELLİKLERİ İÇİN AMPİRİK DENKLEMLER VE POISSON ORANLARI

ÖZET: Bu çalışma, daha önce cam düz örme kumaşların yük-uzama özellikleri üzerine yapılan bir çalışmanın devamı niteliğindedir. Daha önceki çalışmada cam düz örme kumaşların yük-uzama ve yük-enden daralma eğrilerinin üç aşamada gerçekleştiği gösterilmiştir. Bular; a) kumaş uzaması ve yandan daralması (1. aşama), b) iplik uzaması, incilmesi ve deney numunesinin şekil değiştirmesi (2. aşama) ve c) lif uzaması ve incelmesidir (3. aşama). Aynı çalışmada, 1. aşamanın açıklanması için teorik çalışma yapılmış, yük-uzama, yük-yandan daralma eğrileri için basit formüller bulunmuş ve Poisson oranları hesaplanabilmiştir. Teorik çalışmada ilmek başı uzaması, ilk defa, dairesel elastik halkanın uzaması problemi kullanılarak hesaplanmıştır. Bu formülasyon, düz örme kumaşlarda deneysel sonuçlara parabolik regresyon denklemleri yazılabildiği durumlarda sürtünme kuvvetleri ile uzamaya sebep olan dış kuvvetlerin birbirinden ayrıştırılabileceği şeklinde bir metod geliştirilmesinin önünü açmıştır. Önceki çalışmayı temel alan şimdiki çalışmada, Cam ve Aramid teknik iplikleri kullanılarak bu sefer karmaşık atkı örme yapıları için geniş bir deneysel yük-uzama ve yük-yandan daralma eğrilerinin 1. aşamaları incelenmiştir. Deney sonuçlarının regresyon denklemleri yazılmış, bazı sık Aramid örgüleri hariç genellikle parabolik regresyon denklemleri elde edilmiştir. Elde edilen parabolik regresyon denklemleri daha önceki çalışmada düz örgüler için elde edilen denklemler esas alınarak, bahsi geçen çalışmada bulunan 'sürtünme ve iç kuvvetler ile dış kuvvetlerin ayrıştırılması metodu' karmaşık örgüler için de geçerli olduğu kabulü yapılarak yorumlanmış ve yük-uzama ve yük-yandan daralma eğrileri ampirik formüller şeklinde ifade edilmiştir. Bu ampirik formüller kullanılarak yük-uzama oranları ve yük-enden daralma oranlarının hesaplanabildiği yeni bir metod geliştirilmiş ve ayrıntılı olarak irdelenmiştir. Bu yeni çıkarılan ampirik formüller, tabii ki, ilgili mühendislik bilgisayar paket programlarında kullanılabilir.

Anahtar Kelimeler: Atkı örme kumaş, yük-uzama eğrileri, enden daralma, ampirik denklemler, cam lifleri, aramid lifleri, başlangıç uzama oranları, başlangıç enden daralma oranları

Sorumlu Yazar/Corresponding Author: arif.kurbak@deu.edu.tr

DOI: 10.7216/1300759920192611611, www.tekstilmuhendis.org.tr

1. INTRODUCTION

Technical applications of knitted fabrics are increasing day by day. Some technical functions of knitted fabrics depend on the geometry of the employed structure as well as on potential changes in its shape under applied loads. In relation to this, Hepworth [1], MacRory et al [2,3], Popper [4], Shanahan and Postle [5], Hong et al [6] have worked on load-extension properties of plain knitted fabrics in course-wise direction. Hepworth [1], MacRory et al [2,3], Popper [4], Shanahan and Postle [7], Hong et al [6], moreover, have worked on load-extension properties of plain knitted fabrics in wale-wise direction. Most of the aforementioned research, however, applied the non-inflexional elastica theory in modelling the extension of the loop head curve. The lack of those models was that discontinuities occurred between the loop head curve and the rest of the loop curves, hence the models did not completely match the experimental results. Moreover, frictional resistances were not properly considered in those early models. Later on, further research on the geometrical and mechanical properties of technical glass plain knitted fabrics in their dry relaxed [8,9] and loaded [10,11] conditions was conducted by Kurbak. Those works [8,9] pointed out that the dry relaxed technical slack plain knitted fabrics kept their stable shapes by the effect of frictional restrains. When the loop heads were assumed to be circular in shape, the reaction force between the loops could be calculated as

$$\frac{R}{B} = \frac{2 \sin \alpha_{10}}{\rho_{BO}(c_0 \cos \eta_0 + e_{10} \tan \eta_0)} \quad (1)$$

where R is the reaction force. B is the bending rigidity, ρ_{BO} is the radius of the curvature at point B in Figure 1, and $\rho_{BO} = a_0$ can be written. The parameter a_0 , in turn, is the radius of the circular loop head curve and c_0 is the course-spacing at relaxed state. The other geometrical parameters α_{10} , and η are, respectively, the leaning angles of the loop head in the third dimension and the leaning angles of the loop arms in course-wise direction at relaxed state, where the general forms of these angles, α_1 and η , are shown in Figure 1. The parameter e_{10} is the major diameter of the imaginary cylinders at relaxed state, which are illustrated in Figure 1.

In further work, Kurbak [10,11] investigated the load-extension and load-contraction properties of plain knitted glass technical fabrics experimentally and theoretically. The results showed that there were three stages of extensions or contractions namely a) the extension or contraction of the fabric (the first stage), b) the extension or contraction of the yarn along with the shape changes of the samples (the second stage), c) the extension or contraction of the fibres (the third stage). Kurbak then conducted a theoretical work to explain the first stage of extensions or contractions further and obtained the following equations:

When the fabrics were loaded in the wale-wise direction, the relation between the extension rate ϵ_{1W} and the load T_W and also between the contraction rate ϵ_{2W} and T_W were given by

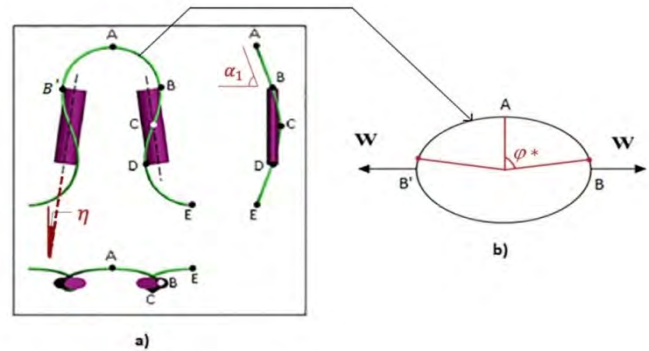


Figure 1: Plain knitted slack fabric model (Kurbak [11]).

$$\epsilon_{1W} = \frac{S_{W20d} - T_W}{(c_0 - S_{W10}) 2R} \quad (2)$$

$$\epsilon_{2W} = \frac{1}{(w_0 + D_W)} \left[-D_W - v(w_0 + 2d)^2 \frac{\sqrt{0.950} \sqrt{T_W/2 + F_{SW}}}{9.672\sqrt{B}} \right] \quad (3)$$

When the fabrics were loaded in the course-wise direction, the relation between the extension rate ϵ_{1C} and the load T_C and also between the contraction rate ϵ_{2C} and T_C were given by

$$\epsilon_{1C} = \frac{1}{(w_0 + D_C)} \left[-D_C + (w_0 + 2d)^2 \frac{\sqrt{1.076} \sqrt{T_C + F_{SC}}}{9.672\sqrt{B}} \right] \quad (4)$$

$$\epsilon_{2C} = -\frac{S_{C20d} - T_C}{(c_0 - S_{C10d}) R} \quad (5)$$

where ϵ_{1W} is the extension rate in the wale-wise loaded samples. ϵ_{2W} is the contraction rate in the course-wise direction under load applied in the wale-wise direction. ϵ_{1C} is the extension rate in the course-wise loaded samples. ϵ_{2C} is the contraction rate in the wale-wise direction under load applied in the course-wise direction.

$$D_W = v(w_0 + 2d)^2 \frac{\sqrt{0.950} \sqrt{F_{SW}}}{9.672\sqrt{B}}$$

$$F_{SW} = 0.405 g.$$

$$S_{W10} = \mu [\sin \alpha_{1,av} - \cos \alpha_{10}] = 0.08705$$

$$S_{W20} = [1 + \mu \sin \alpha_{1,av}] = 1.1954$$

$$D_C = (w_0 + 2d)^2 \frac{\sqrt{1.076} \sqrt{F_{SC}}}{9.672\sqrt{B}}$$

$$F_{SC} = 0.695 g.$$

$$S_{C10} = \mu [\cos \alpha_{10} + v(\sin \alpha_{1,av} - \cos \alpha_{10})] = 0.1516$$

$$S_{C20} = [v + \mu \sin \alpha_{1,av}] = 0.6874$$

Where w_0 and c_0 are the wale-spacing and course-spacing of fully relaxed fabric (global minimum without friction). F_{SW} , F_{SC} , S_{W20d} and S_{C20d} are the frictional forces in Equations (2 - 5) which are applied in dry relaxed state. D_W , D_C , S_{W10d} and S_{C10d} are the differences between the dry relaxed fabric parameters (c , w) and fully relaxed fabric parameters (c_0 , w_0). The indices in Equations (2 - 5) are used as such that c and w are used for the load

application directions, 1 and 2 are used for extension and contraction respectively.

The diameter of the 136 tex glass yarn $d = 0.354 \text{ mm}$ was found. The coefficient of the friction between glass and glass was obtained as $\mu = 0.24$. The bending rigidity $B = 2.87 \text{ gmm}^2$ was used. For Poisson's ratio $\nu = 1/2$ was found for plain knitted fabrics. $\alpha_{10} = 61.159^\circ$ and $\alpha_{1,av} = 51.331^\circ$ were taken for the course-wise loaded samples and $\alpha_{10} = 63.031^\circ$ and $\alpha_{1,av} = 54.71^\circ$ were found for the wale-wise loaded samples. Further parameters are given in Table 1.

It should be noted here that α_{10} was the loop head leaning angle at relaxed fabric state. This angle changed with applying load. The geometrical model of the plain knit fabric was also drawn at the last point of the first stage of the load-extension curve. This point was the fifth point of the dead weights applied. The drawn geometrical model gave a α_{1l} leaning angle value. The average of α_{10} and α_{1l} was then taken as $\alpha_{1,av}$ value.

Table 1. Reference state parameters of glass plain knitted fabric (Kurbak [11]).

Ref. State parameters				Reaction Force
	w_0/d	c_0/d	l/d	$R[g]$
Wale-wise loaded samples	6.751	4.410	22.987	3.840
Course-wise loaded samples	6.763	4.455	23.361	4.328

The values given in Table 1 were calculated theoretically through the geometrical and physical parameters at the relaxed state.

In obtaining Equations (3 and 4): (a) The loop head curves were modelled by using the equation of the extension of a circular ring (see Kurbak [10]) therefore no discontinuities occurred between the loop head curve and the rest of the loop curves during the extension. (b) It was shown that when the experimental quadratic curve fitting equations

$$y = a_1 x^2 + b_1 x + c_1 \quad (6)$$

were written in the form of

$$y = a_1 (x - x_0)^2 + y_0 \quad (7)$$

the y_0 values were the frictional restrains or/and inter fabric jamming forces. Therefore the equations were written in the form of

$$x - x_0 = \frac{\sqrt{(y-y_0)}}{\sqrt{a_1}} \quad (8)$$

and thus the Equations (3 and 4) were obtained.

Where y is the total load applied in a direction (wale-wise or course-wise), x is the sample length (h) for extension, or the minimum fabric width (b_{min}) for contraction.

In the present work, building on Kurbak's [8-11] works that are described above, the first stages of load-extension and/or load contraction properties of some complex weft knitted structures are

studied experimentally. The aim here is to investigate whether empirical equations based on the Equations (2-4) can be found for such complex knitted fabrics as well, based on the assumption that the y_0 values in Regression Equations (7) being frictional restrains and/or fabric jamming forces also applies for complex fabrics. The outcoming equations are expected to be useful for engineering software that are generally used for technical applications of textiles, such as composite reinforcements, stretch sensors, air permeabilities etc. These kinds of applications usually start from dry relaxed fabric conditions; therefore the study particularly focuses on this state. The work, furthermore, is primarily conducted for composite reinforcement applications, therefore high modulus yarns such as E-glass and para-aramid are chosen for the study.

2. EXPERIMENTAL PROCEDURE

- The knitted structures chosen for this study were 1x1 Rib, Milano Rib, Half Cardigan and Full Cardigan Derivative. Knit notations of these fabrics are given in Figures 2a, 2b, 2c and 2d. It should be noted here that due to some spiralities that occurred in the fabrics with Full Cardigan structure itself, the Full Cardigan Derivative structure that is given in Figure 2d was chosen for this work.
- Samples were knitted on a 7 gauge (7 needles per inch) V-bed hand-knitting machine. In order to study the effect of tightness, the samples were knitted at different cam settings of the machine, namely, three different cam settings for 1x1 Rib (R6, R8, and R10), and two different cam settings for Milano Rib (M8 and M10), Half Cardigan (Y8 and Y10) and Full Cardigan Derivative (S8 and S10).
- Two types of yarns were used to knit the samples, namely, 136 tex E-glass yarn (EC9 68 1x2 twisted E-glass yarn) and 168 tex Aramid yarn (Twaron [12], 2012).

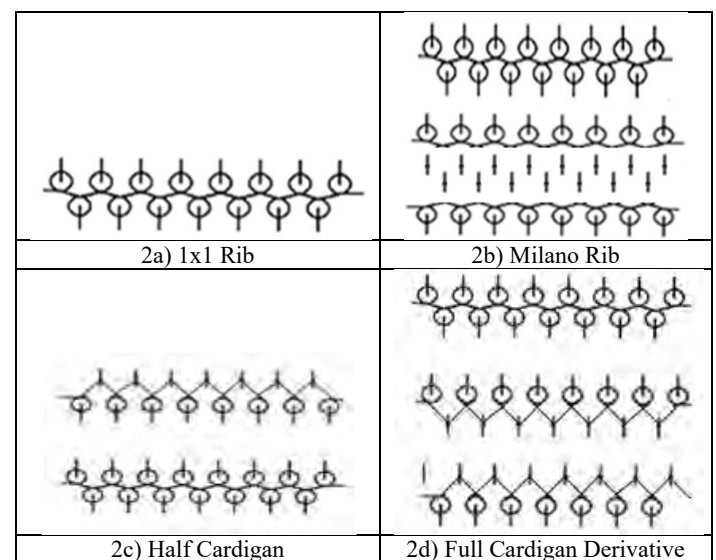


Figure 2. Knit notations of the fabrics chosen in this work

Estimations of the yarn diameters: Kurbak [11] estimated the diameter of 136 tex E-glass yarn as

$$d_g = 1.18 d_{op} = 0.354 \text{ mm} \quad (9)$$

where d_{op} was the yarn diameter in the yarn cross-section calculated by using the open fibre packaging model by Hearle, Grosberg and Backer [13]. It is also known that the yarn diameter can be related to the square root of the yarn tex. When Equation (9) is given in terms of the yarn tex, the equation

$$d_g = 0.03035 \sqrt{\text{Tex}_{\text{glass}}} \quad (10)$$

is obtained. The yarn diameter of 168 tex aramid is estimated here by using the equivalent yarn tex of the aramid in glass as

$$d_a = 0.03035 \sqrt{\frac{168 \times 2.55}{1.44}} \cong 0.5236 \text{ mm} \quad (11)$$

where

$\rho_g = 2.55 \text{ g/cm}^3$ is the density of the glass fibres and $\rho_a \cong 1.44 \text{ g/cm}^3$ is the average density of the aramid fibres.

Estimations of bending rigidities of yarns used: Kurbak [11] used the same 136 tex E-glass yarn and found the bending rigidity B_g for 136 tex E-glass yarn as

$$B_g = 2.87 \text{ gmm}^2 \quad (12)$$

by using an equation given by Lomov and Verpoest [14] for glass yarns as

$$B_g = 1.886 \cdot 10^{-5} \text{ tex}^2 + 1.937 \cdot 10^{-2} \text{ tex} [\text{g mm}^2] \quad (13)$$

On the other hand, Kurbak [15], using a different measuring system, measured the values 2.66 gmm^2 and 18 gmm^2 respectively for the bending rigidities of 136 tex E-glass and 168 tex aramid yarns. Assuming that the ratio $\frac{2.87}{2.66}$ obtained between Lomov and Verpoest's system of measurements and Kurbak's system of measurements for glass yarns is also valid for aramid yarns, the bending rigidity of 168 tex aramid yarn can be estimated as

$$B_a = \frac{2.87}{2.66} \cdot 18 = 19.3483 \text{ gmm}^2 \quad (14)$$

In summary, for the 136 tex E-glass and 168 tex aramid yarns that are used in this work, the estimated yarn diameters that are given in Equations (9) and (11) together with the estimated bending rigidities given in Equations (12) and (14) are used throughout the work.

- Two sets of samples were prepared for each structure, each chosen tightness points, and each yarn. One of the sets was prepared for wale-wise loadings and the other for loadings in the course-wise direction.

The samples were prepared in the following manner:

i) Wale-wise loading samples: The intention was to obtain a $h \times b = 20 \times 10 \text{ cm}$ rectangle as the main measuring area of the samples. Therefore, the sample lengths (h) at dry relaxed fabric condition were chosen in order to fulfil the minimum of 20 cm main sample length plus additional fabric parts above and below the main sample to be used in fixing the jaws of any measurement tester.

Because of the differences in structure and tightness, it was challenging to adjust the sample widths (b) to exact 10 cm in their dry relaxed states. Therefore, a constant knitting zone composed of 35 needles from each bed (from the back and front beds) was set. The sample widths (b), accordingly, were obtained as 10 cm in average.

Because of the high bending rigidities of aramid and glass technical yarns, fabric samples unravel easily. To prevent the unravelling, ten rows of cotton borders were knitted at the beginning and end of each sample. Some examples of E-glass and aramid wale-wise load-extension measuring samples can be seen in Figure 3a. The average sample widths (b), which are obtained by measuring the samples in dry relaxed state at their minimum places, is given in Table 2. A total of five wale-wise loading samples were knitted for each case.

ii) Course-wise loading samples: Again, the abovementioned $h \times b = 20 \times 10 \text{ cm}^2$ main sample area was intended for the course-wise loading samples as well. In this case, a knitting zone constitutes the sample lengths (h) of the course-wise loading samples. Therefore a constant knitting zone of 110 needles on each bed (front and back) was set. Through this setting, it was possible to obtain the minimum sample length of 20 cm as well as the additional fabric parts at the lower and upper sides necessary for fixing the samples in the jaws of any measuring tester. Again, it was challenging to keep the sample widths (b) at exactly 10 cm. Based on the initial tests that were conducted, sufficient numbers of rows of fabric were knitted as the widths (b) of the course-wise loading samples and the intended average sample widths (b) around 10 cm was achieved.

A total of 5 samples per case were knitted to measure the course-wise extension of the fabrics. The averages of the 5 sample widths (b), which were measured at their dry relaxed conditions, are given in Table 2.

To prevent unraveling, 10 rows of cotton borders were knitted at the beginning and at the end of each sample. It was assumed that these cotton borders had neglectable minimal effect on the load-extension measurements.

Some examples of course-wise loading samples are given in Figure 3b.

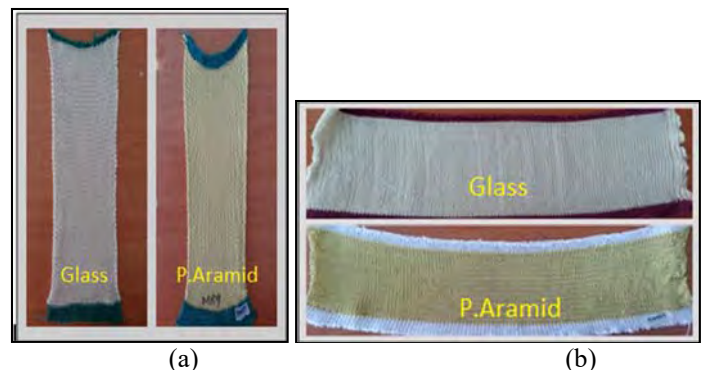


Figure 3. Experimental Samples a) Wale-wise load extension measuring samples, b) Course-wise load-extension measuring samples.

Table 2. The average sample widths (*b*) in cm.

		1x1 Rib			Milano Rib		Half Cardigan		Full Cardigan	
		R6	R8	R10	M8	M10	Y8	Y10	S8	S10
Glass	Wales-wise	9.46	9.8	11.5	8.72	11.54	10.82	11.74	11.5	14.2
	Course-wise	10.08	6.7	8.62	9.18	9.68	9.28	8.96	8.34	8.62
Aramid	Wales-wise	7.76	10.12	12.12	8.86	9.82	11.66	12.1	11.3	13.22
	Course-wise	9.14	9.26	8.54	9.64	10.18	9.46	8.3	8.12	7.14

- For each experimental case, one extra sample was prepared to measure the samples' dimensional properties.

- In total, 216 samples were prepared:

4 types of structure x (2 different tightness value +1 extra tightness value for 1x1 rib) x 2 types of yarn x 2 directions (wale-wise and course-wise) x (5 samples from each case to measure the load-extension properties + 1 extra sample for measuring dimensional properties of the samples) = 216 samples.

- The measurement methods of dimensional properties at dry relaxed fabric condition:

i) Courses per cm (*cpc*) and wales per cm (*wpc*):

After two weeks of dry relaxation on a smooth surface, courses per cm (*cpc*) and wales per cm (*wpc*) were counted with a two-inch square magnifying glass at three different places of the wale-wise loaded samples. The same was done for the course-wise loaded samples. Then, the average value was obtained and divided by 2x2.54 as (*cpc*) and (*wpc*).

In the half cardigan structure, the number of courses on the front side is twice the number of courses on the backside. Thus, in this work, the number of courses on the backside was taken into consideration. To obtain the number of courses on the front side, the number of courses obtained here should be multiplied by two.

ii) Loop length (*l*):

After two weeks of dry relaxation on a smooth surface, areas in the size of 10x5 cm² were pointed out at three different regions

of each sample and these areas were cut out. From each piece, 5 rows were separated and their course lengths (*L*) were measured by hanging 10 g weights below them. With 10 g weight, the curled yarns were observed to be straightened. The average of 3 parts x 5 rows = 15 course lengths (*L*) was divided by the average number of loops (at the back and in the front sides) in a row in order to obtain the loop length (*l*).

Dönmez and Kurbak [16] and also Kurbak and Alpyıldız [17], 2009b showed that the yarn length of a tuck stitch was slightly bigger than the stitch length (*l*) of a normal loop. In the present work, however, if a row is constructed as a combination of tuck stitches and normal stitches, the yarn length of tuck stitches and the yarn length of normal stitches are assumed to be equal. Thus, the average loop length (*l*) was found by dividing the average course length (*L*) by the total number of normal stitches plus tuck stitches in a particular row.

If a structure unit, like the Half Cardigan, has rib rows and rows that contain tuck stitches, the stitch lengths of the two types of rows were given separately.

If a structure unit, like the Milano Rib, is a combination of rib rows and plain knit rows, their stitch lengths were, again, given separately.

The obtained dimensional properties of dry relaxed samples are given in Table 3a for E-glass samples and in Table 3b for Aramid samples.

Table 3a. Dimensional properties of dry relaxed Glass fabric samples

Knitted Structures	Tightness	Loop Length (<i>l</i>) [mm]	Course per cm (<i>cpc</i>)	Wales per cm (<i>wpc</i>)	Mass per unit area g/m ²
1x1 Rib	R6	5.923	9.52	4.69	783.409
	R8	7.330	7.65	3.54	575.587
	R10	9.185	5.37	3.02	460.176
Milano Rib	M8	Rib/Plain 7.815/ 5.807	8.06	3.84	718.239
	M10	Rib/Plain 9.698/ 7.307	6.63	2.86	475.402
Half Cardigan	Y8	Rib/Tuck 7.295/ 7.56	6.32	3.05	842.921
	Y10	Rib/Tuck 9.243/ 9.842	4.8	2.61	678.354
Full Cardigan Derivative	S8	Rib/Tuck 7.463/ 7.739	4.1	3	842.755
	S10	Rib/Tuck 8.860/ 9.378	4	2.3	659.663

Table 3b. Dimensional properties of dry relaxed Aramid fabric samples

Knitted Structures	Tightness	Loop Length(<i>l</i>) [mm]	Course per cm (<i>cpc</i>)	Wales per cm (<i>wpc</i>)	Mass per unit area g/m ²
1x1 Rib	R6	6.620	7.66	3.98	749.002
	R8	7.358	7.49	3.37	691.027
	R10	8.813	5.79	3.31	677.532
Milano Rib	M8	Rib / Plain 7.835/ 6.775	8.03	4.13	866.605
	M10	Rib/Plain 9.769/ 8.805	5.72	3.3	658.282
Half Cardigan	Y8	Rib/Tuck 7.524/ 7.961	5.18	2.88	833.477
	Y10	Rib/ Tuck 8.917/ 9.498	3.36	2.81	682.489
Full Cardigan Derivative	S8	Rib/ Tuck 6.844/ 7.210	6.8	2.9	815.225
	S10	Rib/Tuck 9.007/ 9.804	3.5	2.5	651.702

It should be remembered that the inverse of (*cpc*) and the inverse of (*wpc*) in Tables 3a and 3b are equal to the course-spacing (*c*) and the wale-spacing (*w*) respectively as

$$c = \frac{10}{(cpc)} [mm] \quad (15)$$

$$w = \frac{10}{(wpc)} [mm] \quad (16)$$

• Methods of load-extension and load-contraction measurements:

The load-extension and load-contraction properties of the samples were measured by a special apparatus (Elmalı [18]) seen in Figure 4, since standard methods would not have allowed exploring the load-contraction behaviours of the fabrics in question.

Since technical yarns are too brittle and often break when being fixed in the jaws of load-extension measurement testers, a special friction system was designed to be used at the upper and lower ends of the samples in order to prevent yarn breakages. Load-extension and load-contraction behaviours of the samples were measured by hanging dead weights at the lower friction system given in Figure 4. The dead weights were gradually increased and, at each load level, the length (*h*) and the width (*b_{min}*) at the mid points of the samples were measured with a ruler.



Figure 4. Special apparatus to measure the load-extension properties in this work (Elmalı [18]).

According to the initial plan that was set for this study, the first experiments were in fact devoted to measure all three extension and contraction stages (the first, second, and third stage). Therefore, initially, 12 constant dead weights were arranged as given in Table 4.

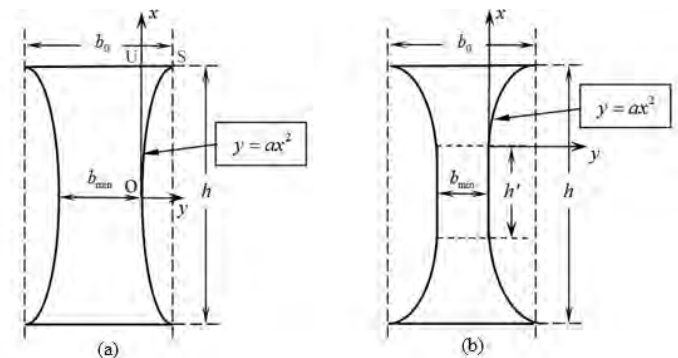


Figure 5. The shape of a sample under loading, a) sample shape for the first stage of extension, b) sample shape for the second and third stages of extension (Kurbak [11]).

During the initial experiments, it was observed that some extension in the fabric parts placed in the inner side of the special friction system shown in Figure 4 inevitably occurred at about the eighth load level. Therefore, despite the original plan, it was later decided that, while continuing to measure all stages of the load-extension and load-contraction curves with 12 constant dead weights, the present work would be devoted only to the first stage of extensions or contractions. The rest of the measurements were solely used for a) predicting the exact load point at which the first stage of extension ended b) figuring out whether all three stages of extensions or contractions can be distinguished in complex structures as in plain knitted structure previously given by Kurbak [11].

Table 4. The dead weights used to measure load-extension and load-contraction properties.

Load Levels	1	2	3	4	5	6
Amount of weight (g)	0	238.4	480	800	1050	1563.33
Load Levels	7	8	9	10	11	12
Amount of weight (g)	2050.5	4050.5	6001.5	8360	10700	12570.5

As a result, load-extension and load contraction curves of all relevant cases were drawn to scale for all 12 dead weights as given in Table 4.

It was observed that:

i) All three stages of extensions and contractions were distinguishable in complex structures as they were in plain knitted fabrics as formerly proven by Kurbak [11]. Some examples of the obtained load extension and load-contraction curves are given in Figures 6a and 6b.

ii) The end point of the first stage is determined to be the 5th load level given in Table 4 for all the cases in question in this study.

iii) Due to the use of a special friction system, no slippages of fabrics occurred in the friction system for the first stages of extensions and contractions.

iv) Since the aim of the present work is focused on the exploration of the first stages of load-extension and load-contraction properties of the cases in question, hereafter, only the first 5 load levels given in Table 4 will be used.

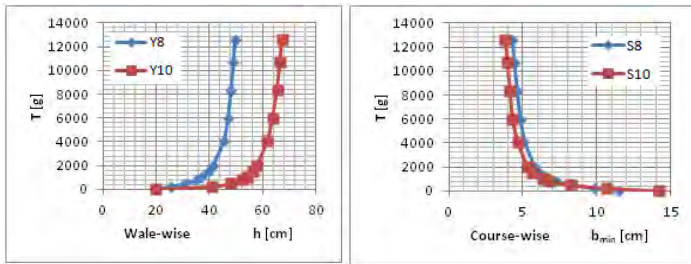


Figure 6. Examples of load-extension and load-contraction results for all three stages (see ref [19]), a) load-extension, b) load-contraction.

3. EXPERIMENTAL RESULTS

Experimentally obtained h and b_{min} values with changing load level T are given at tables in APPENDIX A together with example drawings of load-extension and load-contraction curves for each table.

Regression analyses are applied to all cases in question and given in the form of Equation (6). The constants of Regression Equations (6) are given in Table 5, together with their correlation coefficients R^2 :

As seen in Table 5, the correlation coefficients are very high; therefore, Regression Equations (6) can be used.

For comparison purposes, Regression Equations (6) and their constants given in Table 5 are written in terms of unit structure parameters as follows:

a) For the wale-wise loaded samples

$$T_w = \frac{y}{b(wpc)} \quad (17)$$

is defined, where $b(wpc)$ is the average number of loops on a face of sample width (b). For the case (i) of contraction equations of the wale-wise loaded samples, the equation

$$w_{min} = \frac{x}{b(wpc)} \quad (18)$$

is used, whereas for the case (ii) of extension equations of the wale-wise loaded samples (see Figure 5), the equation

$$c_{av} = \frac{x}{h(cpc)} \quad (19)$$

is used.

It should be noted here that the variable y is the total load applied on a sample, the variable x is the measured length or width of a sample under loading condition. the parameter b and h are the sample width and length respectively at dry relaxed fabric conditions. cpc and wpc are the course per cm and wales per cm of the samples at dry relaxed conditions. T_w , w_{min} and c_{av} values are the calculated wale-wise applied load, minimum wale-spacing (see Figure 5) and average course-spacing of a loop under wale-wise loading conditions.

If the general regression equation is

$$y = a_1x^2 + b_1x + c_1 \quad (20)$$

for the contraction equations of the wale-wise loaded samples

$$T_w = \frac{a_1(b wpc)}{100} w_{min}^2 - \frac{b_1}{10} w_{min} + \frac{c_1}{(b wpc)} \quad (21)$$

change of variables are applied, whereas for the extension equations of the wale-wise loaded samples

$$T_w = \frac{a_1(h cpc)^2}{100 (b wpc)} c_{av}^2 - \frac{b_1(h cpc)^2}{100 (b wpc)} c_{av} + \frac{c_1}{(b wpc)} \quad (22)$$

change of variables are applied, where cpc and wpc are given in Tables 3a and 3b while b parameters are given in Table 2.

Table 5: Constants of Regression Equations (6) together with their correlation coefficients R²

			Contraction, $x = b_{min}$ [cm]					Extension, $x = h$ [cm]			
Structure	Load Direction	Tight	a ₁	b ₁	c ₁	R ²	a ₁	b ₁	c ₁	R ²	
GLASS	1x1 RIB	Wale-Wise	R6 ^{*1}	86.087	-1553	7246.6	0.984	7.3835	-307.92	3453.3	0.9739
			R8	38.067	-739.28	3597.6	0.9923	6.4031	-274.67	2939.4	0.9861
			R10	26.719	-563.73	3958.7	0.978	5.4554	-247.26	2771.8	0.9765
		Course-Wise	R6 ^{*1}	12.312	-391.1	2889.7	0.9873	1.1824	-34.639	410.56	0.9963
			R8	64.499	-789.9	2410.1	0.9634	1.017	-53.209	664.85	0.9817
			R10	57.428	-733.52	2059.5	0.9309	0.9207	-66.554	966.47	0.9589
	MILANO RIB	Wale-Wise	M8	59.717	-1085.1	5131.8	0.9956	7.6744	-301.26	3177.6	0.9943
			M10	21.337	-493.3	2935.7	0.9991	4.1551	-168.37	1727.6	0.9741
		Course-Wise	M8	10.538	-360.36	2601.9	0.9969	5.0279	-160.18	1332.7	0.9966
	HALF CARDIGA N	Wale-Wise	Y8	106.96	-2272.1	12066	0.9978	3.8588	-187.94	2207.5	0.9894
			Y10	121.38	-2655.7	14453	0.9783	4.1865	-208.25	2492.8	0.9875
		Course-Wise	Y8	56.381	-1163.5	5947.4	0.9987	1.4622	-77.269	966.67	0.9799
			Y10	66.541	-1143.6	4908.8	0.9967	1.4782	-97.486	1360.8	0.977
	FULL CARDIGA N	Wale-Wise	S8	30.996	-775.82	4837.1	0.9915	1.9435	-77.354	793.79	0.97
			S10	17.372	-479.63	3322	0.9764	2.0671	-102.84	1239.6	0.9635
Course-Wise		S8	71.31	-1316.5	6027.3	0.9957	1.5107	-81.117	1022.6	0.9786	
		S10	61.012	-986.61	3975.4	0.9891	2.9376	-184.72	2520.6	0.9785	
P.ARAMID	1x1 RIB	Wale-Wise	R6	226.59	-5209	26675	0.9996		724.83	-14496	0.9979
			R8	3.6642	-489.89	4657	0.9756		134.31	-25969	0.9698
			R10	42.727	-1010.2	5994.6	0.9316	3.0278	-118.94	1214.7	0.9419
		Course-Wise	R6		-12919	11810	0.9988		144.71	-2852.3	0.99
			R8		-673.87	6325.1	0.979		95.359	-1892.8	0.9932
			R10		-224.92	1925.3	0.9954	0.72	-27.874	267.3	0.9994
	MILANO RIB	Wale-Wise	M8		-1965.6	17449	0.9937		661.79	-13135	0.9723
			M10	31.111	-997.62	6822.5	0.9939		157.2	-3142.9	0.9835
		(OR)	M10					6.8911	-161.95	513.44	0.9881
		Course-Wise	M8		-1991.5	19266	0.9799		558.83	-11103	0.9842
	M10			-557.73	5734	0.9896		145.16	-2888.4	0.9986	
	HALF CARDIGA N	Wale-Wise	Y8	227.75	-5886.6	37705	0.9987	24.851	-956.3	9200.5	0.9913
			Y10	193.82	-4954.3	31594	0.99	11.109	-427.17	4114.8	0.9882
		Course-Wise	Y8		-656.01	6255.1	0.9894	2.1676	-66.358	478.91	0.9896
			Y10		-335.15	2747.1	0.9781	1.4557	-79.53	1013.7	0.9804
	FULL CARDIGA N	Wale-Wise	S8		-806.24	9201.8	0.9717	5.5094	-145.29	738.45	0.9823
			S10		-341.92	4480	0.9836	13.482	-579.01	6195.7	0.981
		(OR)	S10	46.636	-1433.9	10816	0.9961				
Course-Wise		S8		-772.7	6321.3	0.9907	1.823	-62.759	544.34	0.9853	
		S10		-356.61	2492.1	0.9722	1.6691	-96.791	1271.7	0.9872	
(OR)		S10	70.88	-1165.3	4719.9	0.9963					

*1: The first point is not included in the regression analyses.

It should be noted here that the w_{min} and c_{av} parameters are given in mm, therefore a_1 and b_1 constants in Equations (21) and (22) are also divided by 100 and 10 respectively.

b) On the other hand, for the course-wise loaded samples, the equation

$$T_c = \frac{y}{b(cpc)} \quad (23)$$

is valid. In this category

$$c_{min} = \frac{x}{b(cpc)} \quad (24)$$

for (i) contraction equations and

$$w_{av} = \frac{x}{h(wpc)} \quad (25)$$

for (ii) extension equations should also be considered. Using Equations (23, 24 and 25), the change of variable equations

$$T_c = \frac{a_1(b cpc)}{100} c_{min}^2 - \frac{b_1}{10} c_{min} + \frac{c_1}{(b cpc)} \quad (26)$$

$$T_c = \frac{a_1(h wpc)^2}{100(b cpc)} w_{av}^2 - \frac{b_1(h wpc)}{10(b cpc)} w_{av} + \frac{c_1}{(b cpc)} \quad (27)$$

are obtained to be applied for the contraction equations (i) and for the extension equations (ii) of the course-wise loaded samples respectively.

Where T_c , c_{min} and w_{av} values are the calculated course-wise applied load, minimum course-spacing and average wale-spacing of a loop under the course-wise applied loading conditions.

After applying Equations (21, 22, 26 and 27) in related Regression Equations (6 or 20) through Table 5, the following forms of equations are assumed and applied in accordance with the obtaining of Equation (8) as given in the work of Kurbak [11] for plain knitted glass fabrics.

a) For the wale-wise loaded samples

i) Contraction

$$w_{min} = w_0'' \pm \frac{\sqrt{T_w+m}}{a_2} \quad (28)$$

ii) Extension

$$c_{av} = c_0 \pm \frac{\sqrt{T_w+m}}{a_2} \quad (29)$$

b) For the course-wise loaded samples

i) Contraction

$$c_{min} = c_0'' \pm \frac{\sqrt{T_c+m}}{a_2} \quad (30)$$

ii) Extension

$$w_{av} = w_0 \pm \frac{\sqrt{T_c+m}}{a_2} \quad (31)$$

Here, it should be noted that the m values in Equations (28-31) are assumed to be as frictional restrains and/or fabric jamming forces as were the y_0 values given in Equation (8).

Assuming that the side edges of loaded samples constitute parabolic curves (see Figure 5a) for the first stages of extensions, Kurbak [11] found the following equations to obtain w_{av} and c_{av} in places of w_{min} and c_{min} in Equations (28 and 30), thus

$$w_{av} = \frac{1}{3}w_0' + \frac{2}{3}w_{min} \quad (32)$$

$$c_{av} = \frac{1}{3}c_0' + \frac{2}{3}c_{min} \quad (33)$$

When Equations (32) and (33) are replaced in Equations (28) and (30), the following forms are obtained

$$w_{av} = \frac{2w_0''+w_0'}{3} \pm \frac{\sqrt{T_w+m}}{1.5a_2} \quad (34)$$

$$c_{av} = \frac{2c_0''+c_0'}{3} \pm \frac{\sqrt{T_c+m}}{1.5a_2} \quad (35)$$

These changes of variables are also applied to all of the related Regressions Equations (6) through Table 5, by equalizing the w and c values obtained from Tables 3a and 3b through the Equations (15) and (16) to the w_0' and c_0' in Equations (34) and (35) respectively.

With these final changes, the final forms of Equations (28-31) become as follows:

a) For the wale-wise loaded samples

i) Contraction

$$w_{av} = w_0 \pm \frac{\sqrt{T_w+m}}{a_3} \quad (36)$$

ii) Extension

$$c_{av} = c_0 \pm \frac{\sqrt{T_w+m}}{a_3} \quad (37)$$

b) For the course-wise loaded samples

i) Contraction

$$c_{av} = c_0 \pm \frac{\sqrt{T_c+m}}{a_3} \quad (38)$$

ii) Extension

$$w_{av} = w_0 \pm \frac{\sqrt{T_c+m}}{a_3} \quad (39)$$

where

$$w_0 = \frac{2w_0''+w_0'}{3} \quad (40)$$

$$c_0 = \frac{2c_0''+c_0'}{3} \quad (41)$$

are taken for Equations (36) and (38) and also

$$a_3 = 1.5 a_2 \quad (42)$$

is taken for the same Equations (36) and (38) while a_2 do not change in Equations (37) and (39) as

$$a_3 = a_2 \quad (43)$$

Similar equations as Equations (17-43) are also valid for the cases in which the linear regression equations are applied. The only differences are that the c_{min}^2 , w_{min}^2 , w_{av}^2 and c_{av}^2 parameters should be equalized to zero and the phrases $\sqrt{T_w+m}$ and $\sqrt{T_c+m}$ should be replaced by T_w and T_c all through the Equations (17-43).

The parameters w_0 , c_0 , m and a_3 of Equations (36-39) are given in Table 6 for all cases considered.

When T is equalized to zero in Equations (36-39), two roots are obtained for each case if m is positive. For these cases, the relaxed

fabrics can either be in root 1 condition or in root 2 condition, which are also given in Table 6. If the m parameter is negative, there is no root for T is equal to zero. Therefore, for those cases, 0 (zero) are placed in Table 10. If a regression equation is linear, there is no m value and thus there is only one root. For these cases ‘-’ (dash) are put in places of m and root in Table 6. All these situations are explained further in the next section.

Since it is not useful in practice to have too many equations and also to be able to cover the intermediate tightnesses, some empirical equations are obtained in the next section.

It is seen from Table 6 that the m values are small enough to be considered as frictional restrains and/or fabric jamming forces. Therefore, considering Equation (8) and assuming y_0 values in Equation (8) or the m values in Table 6 as frictional restrains and/or fabric jamming forces is reasonable.

Table 6. The calculated parameters of Equations (36-39) for all the present experimental cases

			c_0, w_0	m	a_3	root
Alai* ¹	w_0	R6	2.0661	-5.4683	9.2703	0
		R8	2.8076	-0.2393	5.4510	0
		R10	3.1287	0.4250	4.5693	2
Alaii	c_0	R6	1.0952	-5.4757	7.7672	0
		R8	1.4018	0.1784	6.5731	1
		R10	2.1100	0.8543	4.2566	1
Albi	c_0	R6	1.4534	2.2529	5.1559	1
		R8	1.2322 (1.4970)	0.1623	8.6245	2
		R10	1.5405	6.1105	7.7338	2
Albii	w_0	R6	1.5616 (2.1322)	-1.1635	1.0412	0
		R8	3.6949	0.6071	0.9973	1
		R10	5.5840	5.1041	0.8518	1
Allai	w_0	M8	2.6770	-6.0390	6.7073	0
		M10	3.5241	-0.7999	3.9805	0
Allaii	c_0	M8	1.2176	-6.6286	7.7173	0
		M10	1.5316	-0.5462	4.6992	0
Allbi	c_0	M8	1.9541	6.4716	4.1885	1
		M10	1.6784	0.2625	4.7693	1
Allbii	w_0	M8	2.0741	-0.7695	2.0020	0
		M10	3.4023	-0.2083	1.5174	0
Alllai	w_0	Y8	3.2385	0.0085	8.9118	2
		Y10	3.6573	2.3877	9.1478	2
Alllaii	c_0	Y8	1.9204	2.0085	4.3222	1
		Y10	2.5908	3.1642	3.5485	1
Alllbi	c_0	Y8	1.7003	0.9413	8.6256	1
		Y10	2.0311	0.5120	8.0103	2
Alllbii	w_0	Y8	4.3315	0.9230	0.9632	1
		Y10	6.3169	5.7310	0.9677	1
AlVai	w_0	S8	3.5294	0.5082	4.9052	1
		S10	4.2268	-0.3499	3.5729	0
AlVaii	c_0	S8	2.4229	-0.7712	1.9462	0
		S10	3.1094	1.2093	2.0126	1
AlVbi	c_0	S8	2.6127	1.4298	7.4070	1
		S10	2.3966	0.3816	6.8799	2
AlVbii	w_0	S8	4.4746	1.9387	1.2611	1
		S10	6.8353	11.1244	1.3427	1
Blai* ¹	w_0	R6	2.5112	-	273.645	-
		R8	2.9673	-	63.558	-
		R10	3.0211	-0.5865	6.21023	0
Blaii	c_0	R6	1.3054	-	359.5424	-
		R8	1.3300	-	58.9942	-
		R10	1.6961	-1.1623	3.1813	0
Blbi	c_0	R6	1.3056	-	193.785	-
		R8	1.3472	-	101.0805	-
		R10	1.7298	-	33.738	-
Blbii	w_0	R6	2.4762	-	16.4528	-
		R8	2.9450	-	9.2681	-
		R10	3.0211	0.0501	0.7988	1

Table 6. The calculated parameters of Equations (36-39) for all the present experimental cases

BIIai	w_0	M8	2.4244	-	294.84	-
		M10	3.0344	-	68.2995	-
BIIaai	c_0	M8	1.2358	-	290.4571	-
		M10	1.7476	-	55.4983	-
BIIbi	c_0	M8	1.2483	-	298.725	-
		M10	1.7618	-	83.6595	-
BIIbii	w_0	M8	2.4054	-	59.6303	-
		M10	3.01485	-	16.4531	-
BIIIai	w_0	Y8	3.7064	9.8962	13.1179	1
		Y10	3.6922	1.9306	12.1769	1
BIIIaai	c_0	Y8	1.8572 (1.5343)	-0.0170	8.9122	0
		Y10	2.8611 (2.8140)	-0.2456	3.8411	0
BIIIbi	c_0	Y8	1.9408	-	98.4	-
		Y10	3.3765	4.5695	5.7436	1
		(or) Y10	2.9515	-	50.2725	-
BIIIbii	w_0	Y8	2.6573	0.5896	1.2114	2
		Y10	4.8606	2.6015	1.2840	1
BIVai	w_0	S8	3.4713	-	120.936	-
		S10	4.4277	6.2299	5.8890	1
		(or) S10	3.9763	-	51.288	-
BIVaai	c_0	S8	0.9695	6.6958	5.5764	2
		S10	3.0676 (2.8414)	0.6345	4.4708	1
BIVbi	c_0	S8	1.4779	-	115.905	-
		S10	3.1453	2.7858	6.3130	1
		(or)	2.8167	-	53.4915	-
BIVbii	w_0	S8	2.9678 (4.0150)	-0.0761	1.0539	0
		S10	5.7990 (5.4429)	5.7989	1.2922	1

*1: A) Glass, B) Aramid, I) 1x1 Rib, II) Milano Rib, III) Half Cardigan, IV) Full Cardigan Derivative, a) Wale-wise loaded samples, b) Course-wise loaded samples, i) Contraction, ii) Extension

4. SUGGESTIONS OF SOME EMPIRICAL EQUATIONS, POISSON'S RATIOS AND CALCULATIONS OF EXTENSION RATES

During the obtaining of empirical equations, the following points were considered.

1. All of the regression equations for glass yarn gave similar equations to Equations (3) and (4), which were obtained for plain knitted fabrics by Kurbak [11]. Therefore, for glass yarn, the following empirical forms of equations should be written:

a) for wale-wise loaded samples

i) contraction

$$w_{av} = w_0 - v_1 \frac{f''(w_0-d)\sqrt{T_w/2+m/2}}{a_4\sqrt{B}} \quad (44)$$

ii) extension

$$c_{av} = c_0 + \frac{f'(c_0)\sqrt{T_w/2+m/2}}{a_5\sqrt{B}} \quad (45)$$

b) for course-wise loaded samples

i) contraction

$$c_{av} = c_0 - v_2 \frac{f''(c_0)\sqrt{T_c+m}}{a_6\sqrt{B}} \quad (46)$$

ii) extension

$$w_{av} = w_0 + \frac{f'(w_0-d)\sqrt{T_c+m}}{a_7\sqrt{B}} \quad (47)$$

2. The Poisson's ratio v_1 in Equation (44) should be equal to the v_2 in Equation (46) as

$$v_1 = v_2 = v \quad (48)$$

During equalizing Poisson's ratios in Equations (44 and 46), f'' functions were so changed that equalities in Equations (44 and 46) were remained the same. Changings of f'' functions were as such that $f' = (v_1/v)f''$ and $f' = (v_2/v)f''$.

3. The constant a_4 in Equation (44) should be equal to a_7 in Equation (47), while the same equality between a_5 and a_6 in Equations (45) and (46) should also be valid:

$$a_4 = a_7 = b_2 \quad (49)$$

$$a_5 = a_6 = b_3 \quad (50)$$

Again during equalizing a_4 and a_7 and also equalizing a_5 and a_6 in Equations (44-47), f' functions were so changed that equalities in Equations (44-47) were remained the same. Changings of f' functions were as such that $f = (b_2/a_4)f'$, $f = (b_2/a_7)f'$, $f = (b_3/a_5)f'$ and $f = (b_3/a_6)f'$.

4. The phrase $(w_0 + 2d)$ in Equations (3) and (4) was created by Kurbak [11] because this phrase was proportional with the loop head radius, a_0 , of the relaxed plain knitted fabrics. Since, in most of the rib structures, the radius of the loop heads, a_0 , proportional with $(w_0 - d)$, assumes that wale jamming conditions occurred, for the extension or contraction in the course's direction, function f in Equations (44) and (47) should depend on $(w_0 - d)$. In this work

$$f(w_0 - d) = (w_0 - d)^n \quad (51)$$

is taken.

On the other hand, there is no such knowledge for wale-wise extensions or contractions, but the function f for Equations (45) and (46) should depend on c_0 because the length (c_0) extends at two ends of a curved part of a loop. Therefore, for f function of Equations (45) and (46), the form

$$f(c_0) = c_0^n \quad (52)$$

is taken.

The f functions given in Equations (51) and (52) are used here for various purposes as such that

i) the upper indices n is used for estimating the intermediate tightnesses,

ii) if any jamming occurs in the fabric in a direction, this can be easily considered by changing the values of upper indices n etc.,

The final empirical parabolic equations to be used in this work are as

a) for wale-wise loaded samples

i) contraction

$$w_{av} = w_0 - v \frac{(w_0 - d)^n \sqrt{T_w/2 + m/2}}{b_2 \sqrt{B}} \quad (53)$$

ii) extension

$$c_{av} = c_0 + \frac{(c_0)^n \sqrt{T_w/2 + m/2}}{b_3 \sqrt{B}} \quad (54)$$

b) for course-wise loaded samples

i) contraction

$$c_{av} = c_0 - v \frac{(c_0)^n \sqrt{T_c + m}}{b_3 \sqrt{B}} \quad (55)$$

ii) extension

$$w_{av} = w_0 + \frac{(w_0 - d)^n \sqrt{T_c + m}}{b_2 \sqrt{B}} \quad (56)$$

5. For aramid fabrics, most of the regression equations are linear in forms as

$$w_{av} = w_0 \pm \frac{T}{b_2} \quad (57)$$

$$c_{av} = c_0 \pm \frac{T}{b_2} \quad (58)$$

The form of Equations (57) and (58) obtained for aramid fabrics can best be explained by using Equations (55) of Kurbak's work [11] for plain knitted fabrics as such that Equation (55) in Kurbak's work [11] was as

$$T_c + F_{sc} = \frac{2B}{3a_0^2} 8.770 (x - 1)^2 \quad (59)$$

where

$$x = \frac{a}{a_0} \cong \frac{w_{av} + 2d}{w_0 + 2d} \quad (60)$$

When Equation (59) is opened up, the equation

$$T_c + F_{sc} = \frac{2B}{3a_0^2} 8.770 (x^2 - 2x + 1) \quad (61)$$

is obtained. Since the bending rigidity, B , of aramid is high as given in Equation (14), the inclination angles of parabolic curves between T and w_{av} are very high; thus, the arms of the parabolic curves obtained for this yarn are extended along which are near the vertical line as given in Figure 7. Because of these higher inclination angles of parabolic curves, the values of w_{av} and w_0 becomes too close to each other, and, thus, x^2 in Equations (61) becomes as

$$x^2 = \frac{a^2}{a_0^2} \cong \frac{(w_{av} + 2d)^2}{(w_0 + 2d)^2} \approx 1 \quad (62)$$

When Equations (62) is replaced in Equation (61), an equation is obtained as

$$T_c + F_{sc} = -\frac{2B}{3a_0^2} 8.770 (2x - 2)$$

and thus

$$T_c + F_{sc} = -b'2B(x - 1) \quad (63)$$

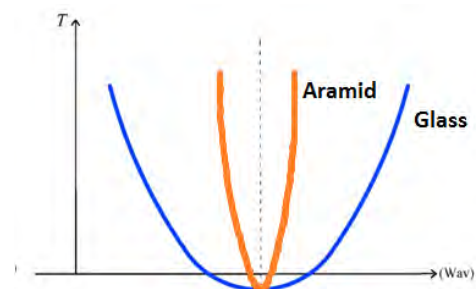


Figure 7. Comparison of parabolic curve fittings of load-extension properties of aramid and glass samples.

It is thought that this must be one of the reasons for obtaining linear regression equations for aramid fabrics. One more reason for obtaining linear regression equations for aramid fabrics will be given later in this section.

As a result of the above discussion, the following forms of empirical equations are used for linear equations of aramid fabrics:

a) for wale-wise loaded samples

i) contraction

$$w_{av} = w_0 - v \frac{(w_0-d)^n T_w}{b_2(2B) \cdot 2} \quad (64)$$

ii) extension

$$c_{av} = c_0 + \frac{c_0^n T_w}{b_3(2B) \cdot 2} \quad (65)$$

b) for course-wise loaded samples

i) contraction

$$c_{av} = c_0 - v \frac{c_0^n}{b_3(2B)} T_c \quad (66)$$

ii) extension

$$w_{av} = w_0 + \frac{(w_0-d)^n}{b_2(2B)} T_c \quad (67)$$

According to the above points, the empirical equations were obtained by the method of trial and error, and they are given in APPENDIX B.

It should be noted here that Empirical Equations in APPENDIX B include one more parameter called 'a'. This parameter is included to equalize two different Poisson's ratios in one structure. The parameter, *a*, is put wherever it is necessary in the equations.

To be able to apply Equations in APPENDIX B, the parameter, *m*, in the equations should also be estimated and discussed further as given below:

i) if the parameter, *m*, is negative

If the parameter, *m*, in an equation is negative and when the external load *T* is set to zero, the square root in the equation becomes irrational. It is thought that these kind of structures are jammed structures, and some of the external loads are spent to overcome these jamming forces. The amounts of inner fabric forces are equal to *m*; therefore the equation

$$T_0 = m \quad (68)$$

should be valid where *T*₀ is the external load to overcome the inner fabric force.

In this situation, an equation in the form

$$w_{av} = w_0 \pm \frac{(w_0-d)^n \sqrt{T_i+m}}{b_2 \sqrt{B}} \quad (69a)$$

$$c_{av} = c_0 \pm \frac{c_0^n \sqrt{T_i+m}}{b_2 \sqrt{B}} \quad (69b)$$

has no root when *T*_i is equal to zero as seen in Figure 8.

It is not difficult to conclude that, if an extension equation has a minus *m* value, the load-extension curve would follow the route which is given in Figure 9a. Again, if a contraction equation has minus *m* value, it should take the route as given in Figure 9b.

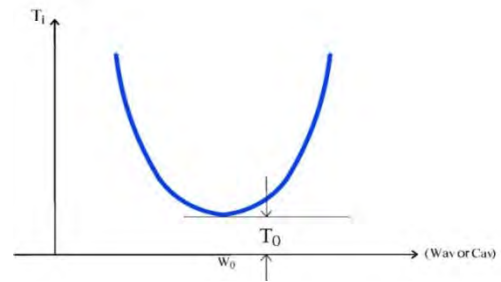


Figure 8. Parabolic curve fittings of load-extension properties of knitted fabrics for negative *m* values in Equations (69a and 69b).

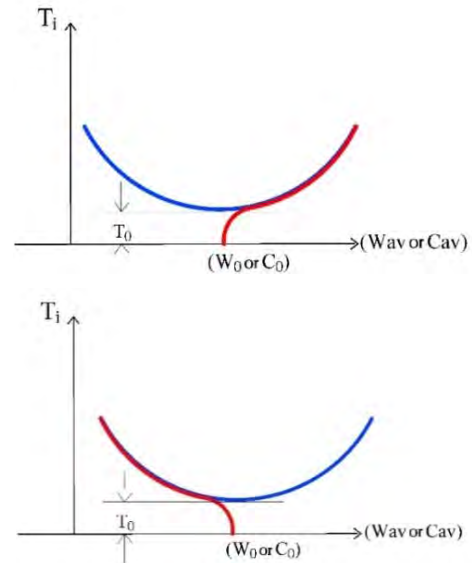


Figure 9. Possible parabolic curve fittings for a) load-extension and b) load-contraction results when the parameter *m* is negative in Equations (69a and 69b).

For these kind of structures, when a load-extension or a load-contraction equation is given in the form as

$$(w_{av} \text{ or } c_{av}) = (w_0 \text{ or } c_0) \pm D_{ii}(T_i + m) \quad (70)$$

practically obtained *w*'₀ or *c*'₀ values should be equal to *w*₀ and *c*₀ values in Equation (70). The rate of extensions or contractions can be given for the negative *m* case in the form as

$$\varepsilon = \frac{(w_{av} \text{ or } c_{av}) - (w_0 \text{ or } c_0)}{(w_0 \text{ or } c_0)} = \mp \frac{D_{ii}(T_i + m)}{(w_0 \text{ or } c_0)}; \text{ for } T_i \geq |m| \quad (71)$$

The cases AIai → (R6, R8), AIaii → (R6), AIbii → (R6), AIiia → (M8, M10), AIiiai → (M8, M10), AIiibii → (M8, M10), AIVai → (S10), AIVaii → (S10) in E-glass fabrics have these kinds of load-extension or load contraction curves (see Figure 10a).

On the other hand, in spite of the linear regression equations that are applied, these kinds of load-extension or load contraction curves can be distinguished in some of the aramid fabrics such as BIai → (R8, R10), BIaii → (R8, R10), BiBi → (R8), BiBii → (R6, R8), BIiia → (M8, M10), BIiiai → (M8, M10), BIiibi → (M8), BIiibii → (M8), BIiia → (Y8, Y10), BIiibi → (Y8), BIVai → (S8), BIVaii → (S8), BIVbi → (S8) (see Figure 10b).

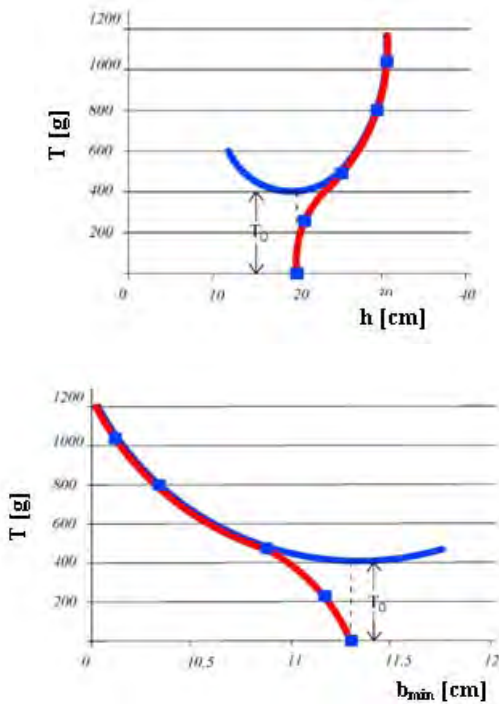


Figure 10. a) The load-extension results of wale-wise extended glass 1x1 rib structure knitted with 6 cam setting and parabolic curve fitting, b) the load-contraction results of wale-wise extended aramid full cardigan derivative sample knitted with an 8 cam setting and parabolic curve fitting.

The diameter of the aramid yarn was $d = 0.5236 \text{ mm}$ while the diameter of the E-glass yarn was $d = 0.354 \text{ mm}$. Therefore, the aramid fabric samples obtained here were tighter than the E-glass samples. Since the jamming forces occur in tight fabrics, most of the load-extension or load-contraction curves of the aramid fabric samples would have minus m values if they could be written in parabolic form. It is thought that this is the other reason to obtain linear regression equations in load-extension or load-contraction curves of the aramid fabrics in addition to the reason given earlier in this section. It can be understood that, although the linear regression equations are applied, some of the aramid load-extension or load-contraction curves for the first stage are actually combinations of two different regions, one of which is the T_0 region and the other is the parabolic region, as seen in Figure 10b:

ii) If the parameter m is positive

For this condition there are two roots of the parabolic equations in the forms as

$$(w_{av} \text{ or } c_{av}) = (w_0 \text{ or } c_0) \pm \frac{[(w_0-d)^n \text{ or } c_0^n] \sqrt{T_i+m}}{b_2 \sqrt{B}} \quad (72)$$

when T is equal to zero. These roots (for the $T_w/2$ and w_{av} relationship, for example) is shown in Figure 11.

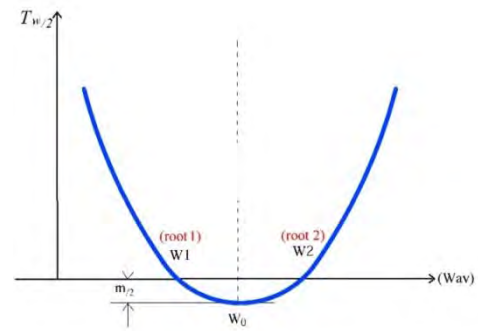


Figure 11. Parabolic curve fittings of load-extension properties of knitted fabrics for positive m values in Equations (69a and 69b).

For further explanation, regression equations to obtain these roots for a fabric sample are written in the form as

a) wale-wise loaded samples

i) contraction

$$w_{1,2} = w_0 \pm D_{2w}(m/2) \quad (73)$$

ii) extension

$$c_{1,2} = c_0 \pm D_{1w}(m/2) \quad (74)$$

b) course-wise loaded samples

i) contraction

$$c_{1,2} = c_0 \pm D_{2c}(m) \quad (75)$$

ii) extension

$$w_{1,2} = w_0 \pm D_{1c}(m) \quad (76)$$

It should be noted here that the minus signs in Equations (73-76) stand for root 1 while plus signs stand for root 2 where

$$D_{2w}(m/2) = v \frac{(w_0-d)^n \sqrt{m/2}}{b_2 \sqrt{B}} \quad (77)$$

$$D_{1w}(m/2) = \frac{c_0^n \sqrt{m/2}}{b_3 \sqrt{B}} \quad (78)$$

$$D_{2c}(m) = v \frac{c_0^n \sqrt{m}}{b_3 \sqrt{B}} \quad (79)$$

$$D_{1c}(m) = \frac{(w_0-d)^n \sqrt{m}}{b_2 \sqrt{B}} \quad (80)$$

can be given for the terms in Equations (73-76). Equations (77-80), in turn, should be evaluated from Empirical Equations in APPENDIX B for the case considered.

Some more definitions are given here to be used in the rest of the work as

$$D_{2w}(T_w/2 + m/2) = v \frac{(w_0-d)^n \sqrt{T_w/2+m/2}}{b_2 \sqrt{B}} \quad (81)$$

$$D_{1w}(T_w/2 + m/2) = \frac{c_0^n \sqrt{T_w/2+m/2}}{b_3 \sqrt{B}} \quad (82)$$

$$D_{2c}(T_c + m) = v \frac{c_0^n \sqrt{T_c+m}}{b_3 \sqrt{B}} \quad (83)$$

$$D_{1c}(T_c + m) = \frac{(w_0-d)^n \sqrt{T_c+m}}{b_2 \sqrt{B}} \quad (84)$$

where Equations (81-84) are used for wale-wise loaded contraction, wale-wise loaded extension, course-wise loaded contraction and course-wise loaded extension respectively.

The evaluations of Equations (81-84) again should be done by using Empirical Equations in APPENDIX B for the case considered.

As analysed in the work of Kurbak [11] the main reason for obtaining the two roots is because of friction resistances which are applied in the dry relaxed fabrics. In the actual situation, the fabric in a dry relaxed state can either be in root 1 (w_1 or c_1) condition or in root 2 (w_2 or c_2) condition.

As a result of the above discussion, to be able to use Empirical Equations in APPENDIX B, w_0 and c_0 values should be known. These values, in turn, can be obtained by using Equations (73-76). The unknown parameters m in Equations (73-76) should be estimated first for obtaining w_0 and c_0 values for the intermediate tightness points along with which root should be taken as the starting point of extension or contraction (root 1 or root 2).

The parameters, m , are estimated and the pattern of the starting root of each curve for E-glass fabric samples were searched assuming that this present pattern is repeatable. and thus the same pattern could be obtained in future works. This work is given as in the following:

- The tightness, l/d , for each case is calculated first using Table 3a and Equation (9). During these calculations, the plain knit row of the unit cell of Milano Rib, the rib row of the unit cell

of Half Cardigan and the rib row of the unit cell of Full Cardigan Derivative Structure are used.

- The parameters, m , given in Table 6 and l/d are drawn in the graphical forms as seen in Figures 12a and 12b for 1x1 rib; in Figures 13a and 13b for Milano Rib; in Figures 14a and 14b for Half Cardigan; and in Figures 15a and 15b for Full Cardigan Derivative structures.
- Assuming linear relations between m values and tightness l/d values, a pattern of m values for each structure was obtained and is given in the related figures (Figures 12-15).
- The starting roots of extensions and contractions are also shown on these graphical representations by putting (-) for root 1, (+) for root 2, and (.) for negative m values on top of each case.

When Figures (12-15) are searched, it is seen that the negative m values are seen to be obtained mainly for tight fabrics.

It should be added that the glass milano rib structure samples have mostly negative m values. The reason may be the tighter plain knit rows of the unit cell of the milano rib. The rib row and the plain knit rows of the unit cell of the milano rib have been knitted in the same cam setting which is against the experience that the normal tightness of plain knit requires a higher cam setting than the normal cam settings of the 1x1 Rib.

- The relaxed fabrics which are being in root 1 or root 2, is mostly effective on the extension rates and the contraction rates. Since the rate of extension and the rate of contraction are preferred in places of the extension and the contraction themselves in practice, calculations of the extension rate and contraction rate are explained briefly as follows:

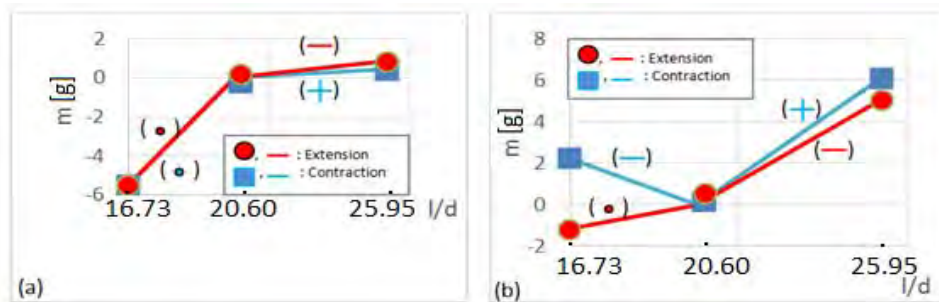


Figure 12. The parameter m vs. l/d for 1x1 Rib, a) Wale-wise loaded samples, b) Course-wise loaded samples.

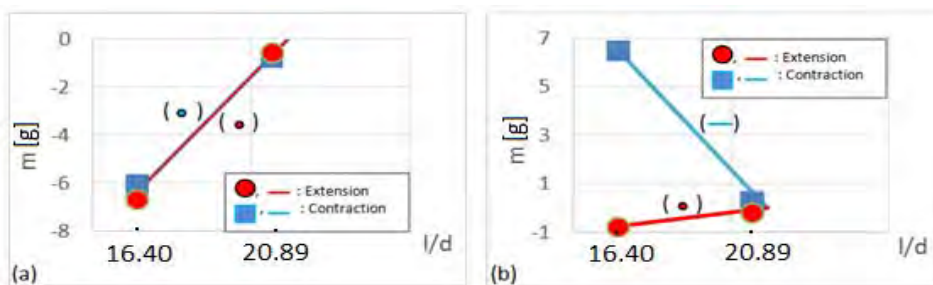


Figure 13. The parameter m vs. l/d for milano rib, a) Wale-wise loaded samples, b) Course-wise loaded samples.

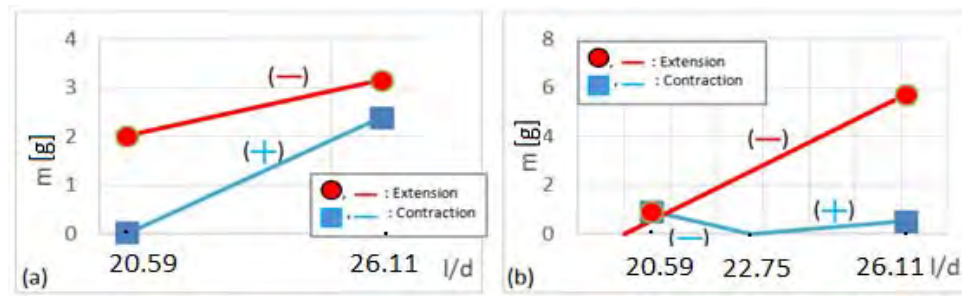


Figure 14. The parameter m vs. l/d for half cardigan, a) Wale-wise loaded samples, b) Course-wise loaded samples.

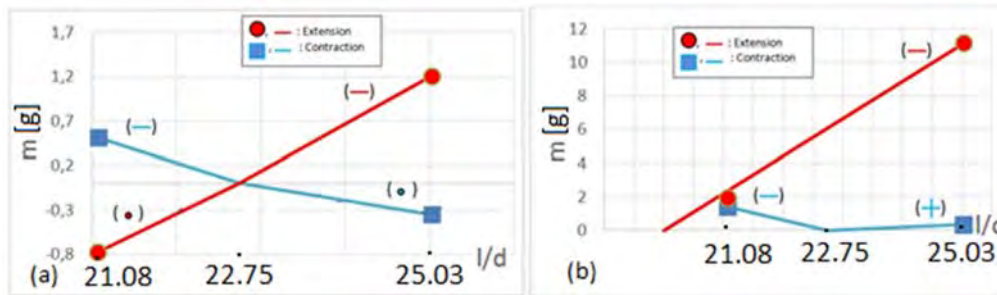


Figure 15. The parameter m vs. l/d for full cardigan derivative, a) Wale-wise loaded samples, b) Course-wise loaded samples.

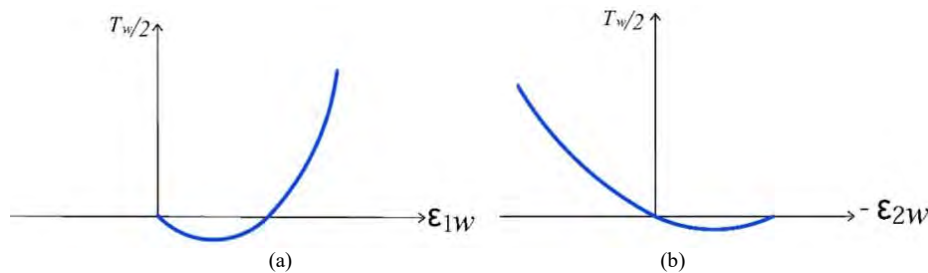


Figure 16: Load-extension and load-contraction curves when the fabric is in rroot 1 condition, a) load-extension curve, b) load-contraction curve.

i) If the relaxed fabric state is in root 1, for example, for the contraction of the wale-wise loaded samples, the contraction rate would be as

$$\epsilon_{2w} = \frac{[w_{av} - (w_0 - D_{2w}(m/2))]}{[w_0 - D_{2w}(m/2)]} = \frac{D_{2w}(m/2) - D_{2w}(T_w/2 + m/2)}{w_0 - D_{2w}(m/2)} \quad (85)$$

If the relaxed fabric state is in root 1, for example, for the extension of the wale-wise loaded samples, the extension rate would be as

$$\epsilon_{1w} = \frac{c_{av} - (c_0 - D_{1w}(m/2))}{c_0 - D_{1w}(m/2)} = \frac{D_{1w}(m/2) + D_{1w}(T_w/2 + m/2)}{[c_0 - D_{1w}(m/2)]} \quad (86)$$

The relations between $T_w/2$ and ϵ_{1w} and between $T_w/2$ and ϵ_{2w} would be as in Figures 16a and 16b, respectively.

ii) If the relaxed fabric state is in root 2 condition, for the contraction of the same wale-wise loaded sample, the contraction rate would be as

$$\epsilon_{2w} = \frac{w_{av} - (w_0 + D_{2w}(m/2))}{[w_0 + D_{2w}(m/2)]} = \frac{-D_{2w}(m/2) - D_{2w}(T_w/2 + m/2)}{w_0 + D_{2w}(m/2)} \quad (87)$$

If the relaxed fabric state is in root 2 condition, for the extension of the same wale-wise loaded sample, the extension rate would be as

$$\epsilon_{1w} = \frac{c_{av} - (w_0 + D_{1w}(m/2))}{c_0 + D_{1w}(m/2)} = \frac{-D_{1w}(m/2) + D_{1w}(T_w/2 + m/2)}{c_0 + D_{1w}(m/2)} \quad (88)$$

The relations between $T_w/2$ and ϵ_{1w} and between $T_w/2$ and ϵ_{2w} would be as in Figures 17a and 17b.

Very similar equations as Equations (85-88) and very similar curves as in Figures (16-17) are obtained for the course-wise loaded samples, as well.

It can be seen from the above discussion that the extension rates and/or the contraction rates are different according to the relaxed fabrics being in root 1 or root 2. Using the present experimental results, the equations of m values in terms of tightness (l/d) (assuming linear relations), the starting roots of the relaxed fabrics, and the contraction or the extension rates for glass fabrics are given in APPENDIX C.

To complete the work, the calculated load-extension and load-contraction rates are compared with the experimentally obtained load-extension and load-contraction rates in Figures 18-26 for all the structures, tightness, and types of yarns used in this work.

During obtaining the theoretical load-extension curves in Figures 18-26, the m , c_0 , and w_0 values are taken from Table 6. According to the roots given in Table 6, similar equations as in Equation (71, 85-88) are calculated to obtain the extension or contraction rate values. As noted above, example calculations of extension and contraction rates are also given in APPENDIX C for the glass samples.

During obtaining the experimental extension or contraction rates, Tables in APPENDIX A are used as

$$\varepsilon_2 = \frac{b_{\min(i)} - b_0}{1.5 b_0}; \quad (i = 1 \text{ to } 5) \quad (89)$$

$$\varepsilon_1 = \frac{h_i - h_0}{h_0}; \quad (i = 1 \text{ to } 5) \quad (90)$$

It should be noted here that the contractions are measured in the middle of the samples as b_{\min} . In order to obtain b_{av} values, the side edges of the samples are assumed to be as in Figure 5a in this work, and similar equations as Equations (34-35) are used for obtaining b_{av} values. Therefore, a dividing factor 1.5 exists in Equation (89).

The load applied, T , are calculated by dividing the total loads given at the Tables in APPENDIX A by the average number of loops on a face of the cross-section of fabric that carries out the total loads as

$$T_w = \frac{\text{Total wale-wise Loads (see Tables 5 and 7)}}{b \text{ (wpc)}} \quad (91)$$

$$T_c = \frac{\text{Total course-wise Loads (see Table 6 and 8)}}{b \text{ (cpc)}} \quad (92)$$

The applied loads T_w and T_c given in Equations (91-92) are used for obtaining the theoretical calculations of extension and contraction rates as well as for obtaining the experimental load-extension and load-contraction results.

It should be said further that $b \text{ (wpc)}$ and $b \text{ (cpc)}$ in Equations (91-92) are the average number of loops on one face of the samples. The chosen faces were explained during obtaining (wpc) and (cpc) parameters by using Equations (15-16). These definitions of applied loads makes easier to obtain the carried load by a unit cross-sections of fabrics at any structures by having $T_w \text{ (wpc)}$ [g/cm] and $T_c \text{ (cpc)}$ [g/cm] and so on.

In some of the cases, c_0 and w_0 values given in Table 6 do not give the calculated extension and/or contraction rates correctly, so the drawn curves do not follow the experimental points. For these cases some suitable c_0 and/or w_0 values are calculated to fit the experimental points. These calculated new c_0 and/or w_0 values are given in Table 6 in brackets. They may be due to five experimental points which are less for obtaining the correct c_0 and/or w_0 values.

In some of the tight fabric cases, the calculated curves do not follow the experimental points. These discrepancies can be explained as follows; for example, for the glass 6 cam setting tight fabrics, the first point was put out of the regression equation. It was later seen that the second point in the 6 cam setting and the first point in the 8 cam setting of the 1x1 rib glass fabric should also be put out of the regression equations as shown in Figure 10. This kind of discrepancy is also the result of fewer experimental points since, if the second experimental point in the 6 cam setting of the glass fabrics were also left out of the regression equations, only three point would be left for a quadratic curve fitting.

In spite of some discrepancies mentioned above, it is seen that Empirical Equations in APPENDIX B can be used to estimate the extension and the contraction rates for a given load value for any kind of complex knitted structure at any tightness.

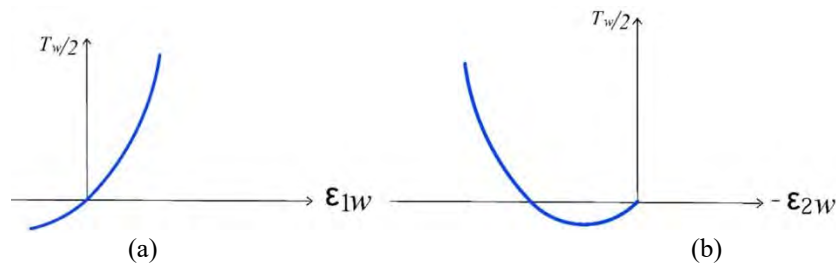


Figure 17: Load-extension and load-contraction curves when the fabric is in root 2 condition, a) load-extension curve, b) load-contraction curve.

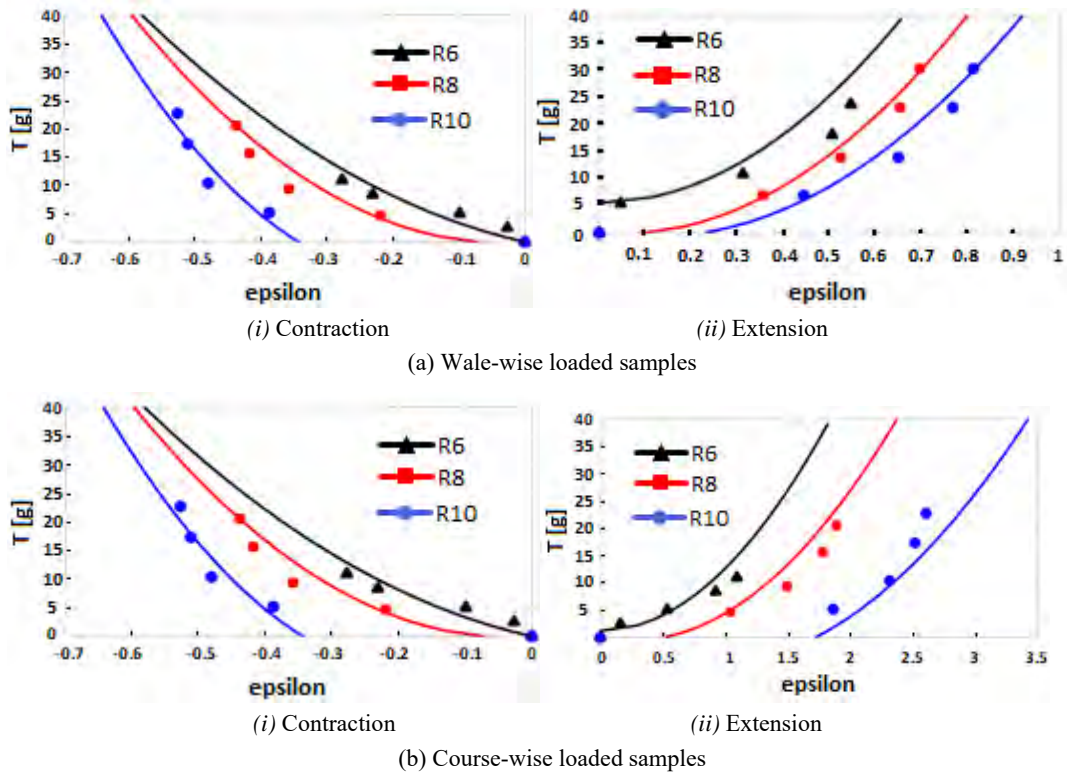


Figure 18: Glass 1x1 rib load-extension results and empirical equations.

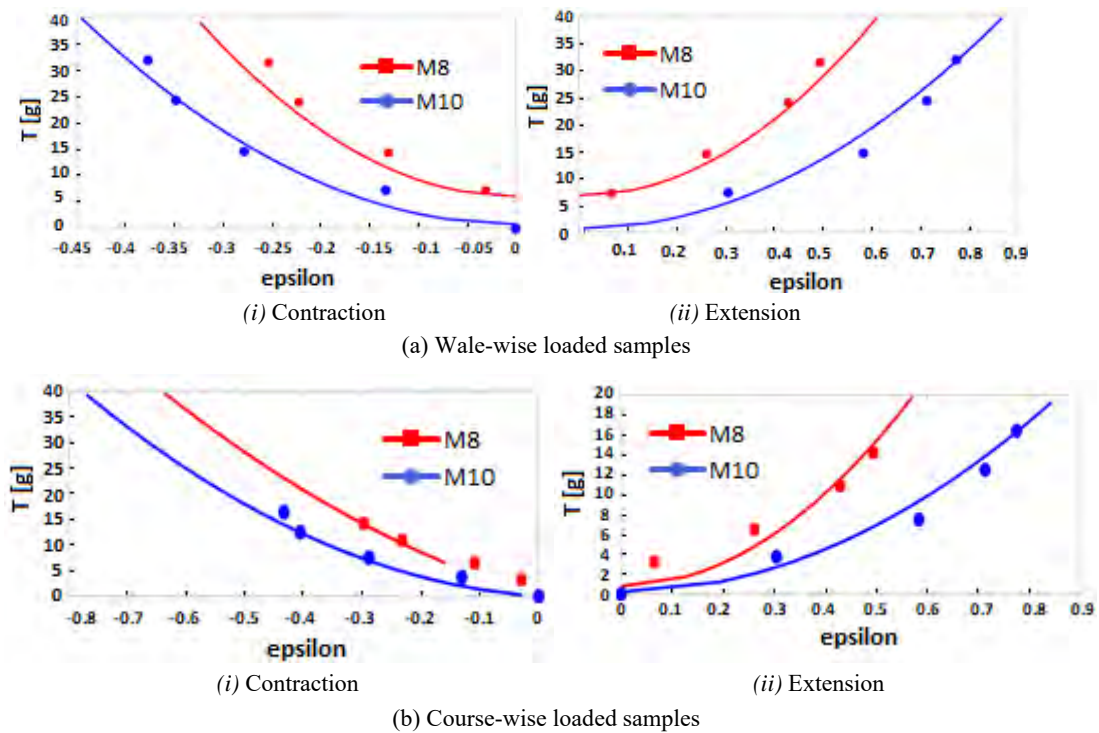


Figure 19: Glass milano rib load-extension results and empirical equations.

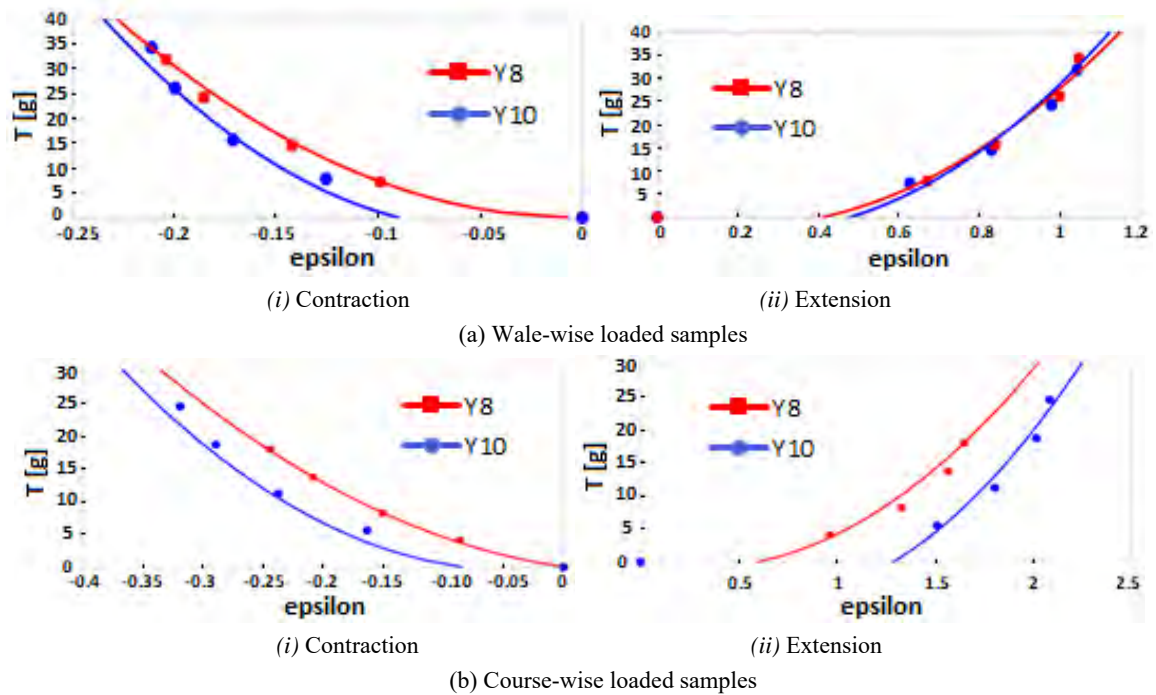


Figure 20: Glass half cardigan load-extension results and empirical equations.

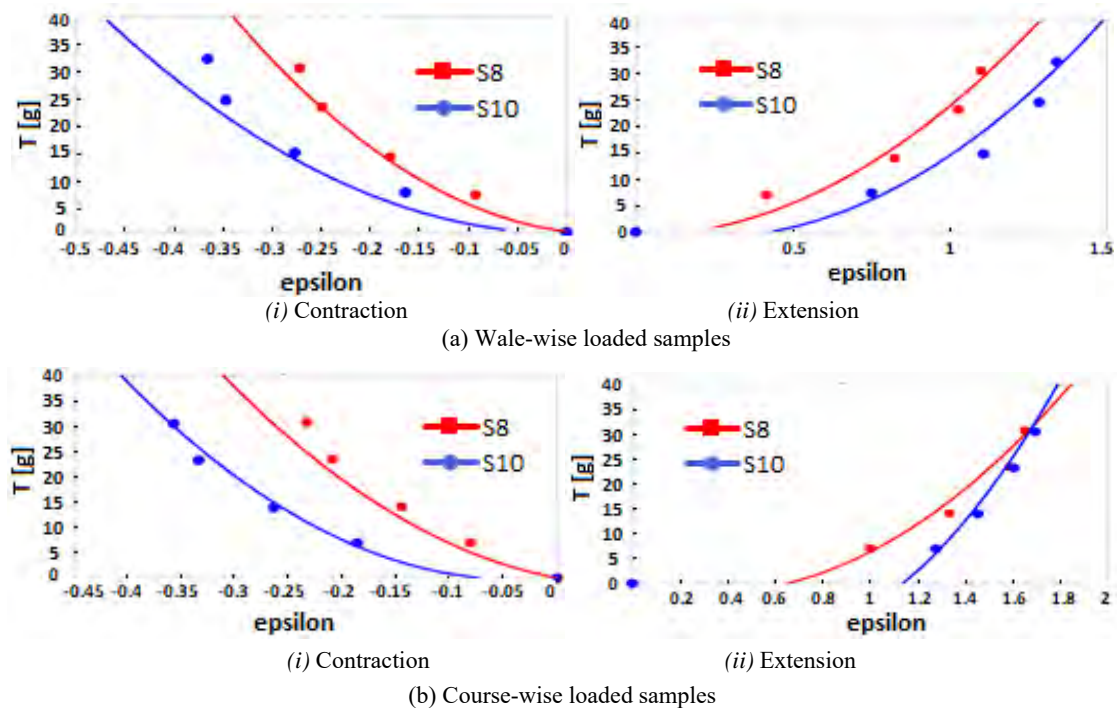


Figure 21: Glass full cardigan load-extension results and empirical equations.

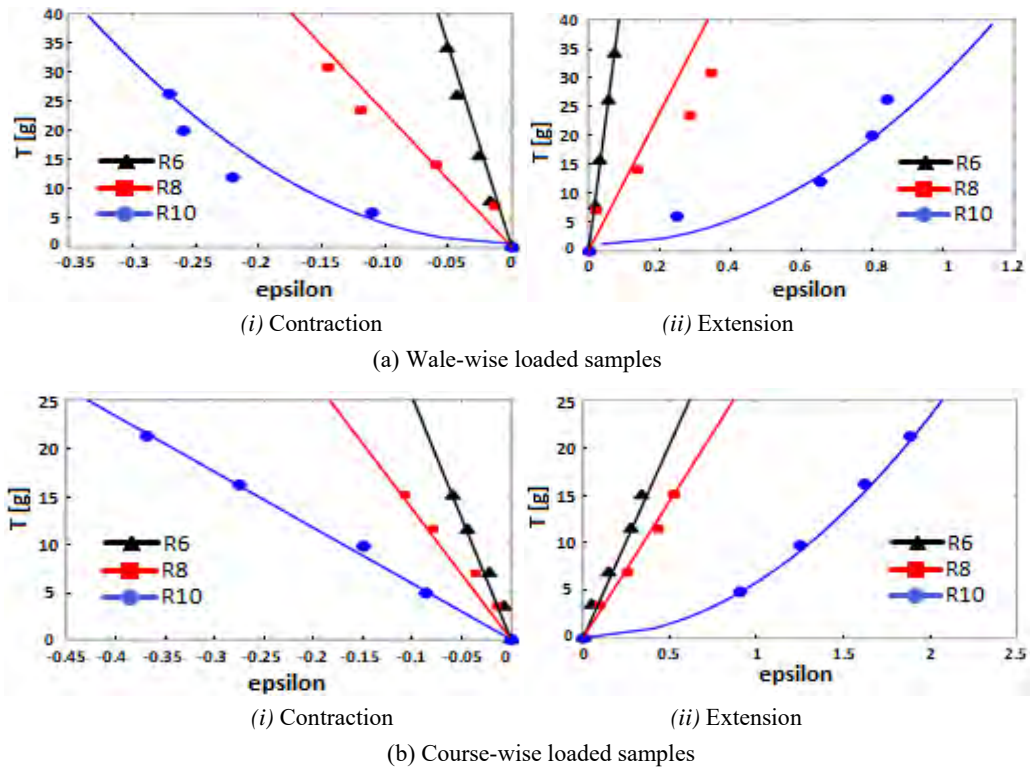


Figure 22: Aramid 1x1 rib load-extension results and empirical equations.

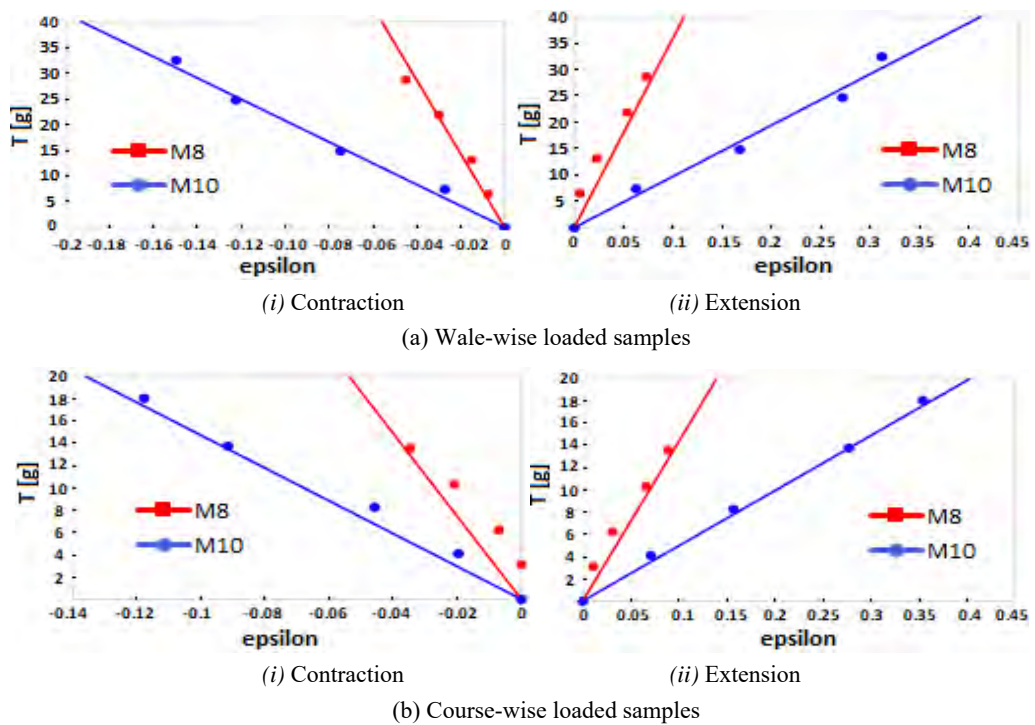


Figure 23: Aramid milano load-extension results and empirical equations.

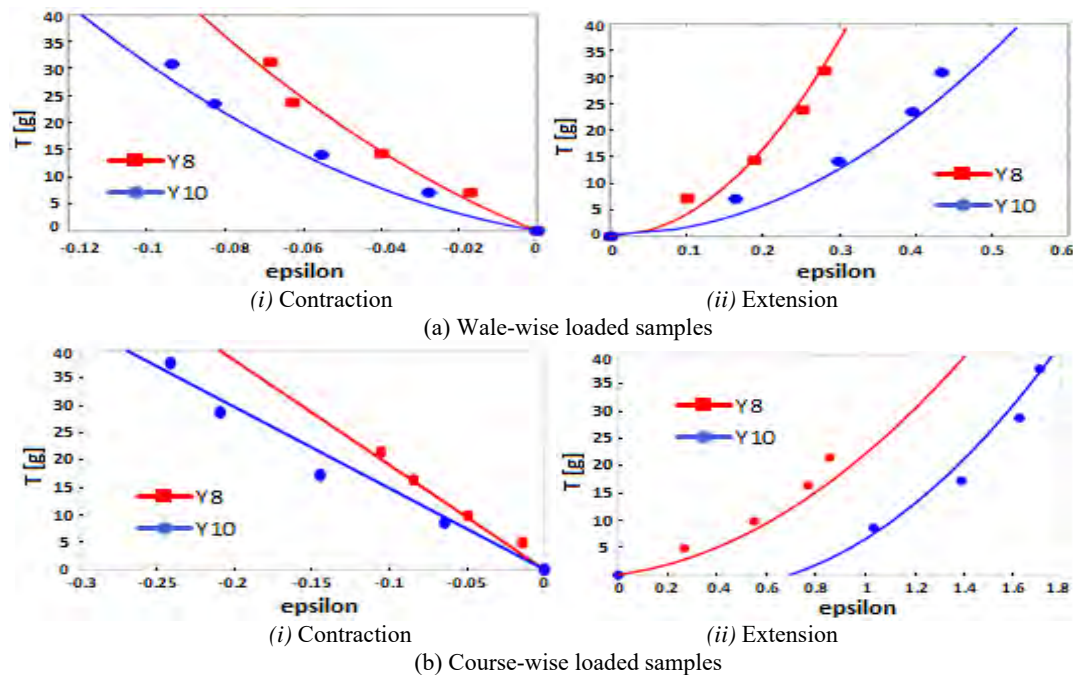


Figure 24: Aramid half cardigan load-extension results and empirical equations.

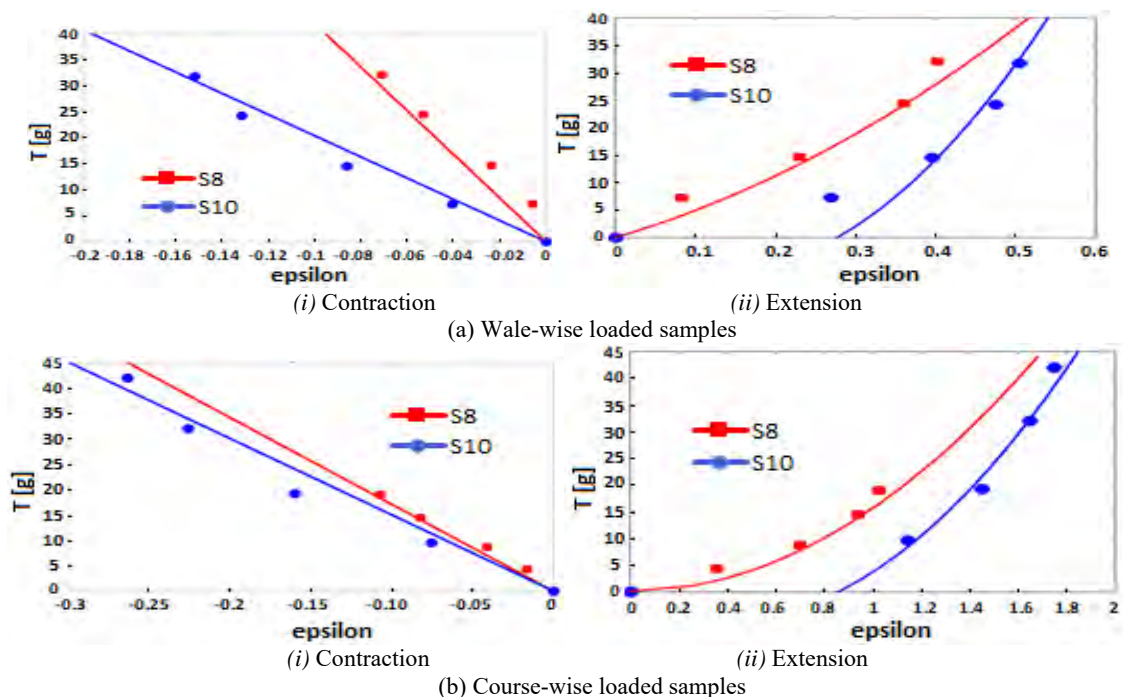


Figure 25: Aramid full cardigan load-extension results and empirical equations.

5. RESULTS AND DISCUSSION

Results of the initial load-extension and load-contraction properties of complex weft knitted fabrics will be given in comparison with the same properties of plain knitted fabric which was given by Kurbak [11] such that:

i) For the extension and contraction in fabric length direction of plain knitted glass fabric, linear regression equations with higher correlation coefficients could be applied while they were quadratic curve fittings for the fabric width directions. For the extension and

the contraction in both directions for complex weft knitted glass fabrics, however, quadratic curve fittings could be applied with higher correlation coefficients. It may be because of the loop arms which are nearly two dimensional curves for plain knitted fabrics while they are three dimensional for complex weft knitted structures.

ii) Mainly three kinds of quadratic curve fittings are obtained for complex weft knitted fabrics as given in schematic Figures 26a, 26b and 26c.

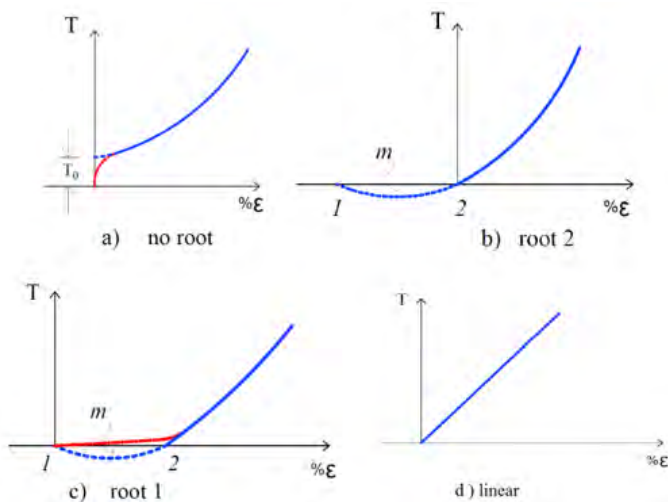


Figure 26. Schematic drawings of curve fittings obtained for load against extension rates (T vs. $\% \epsilon$) of complex weft knitted structures a) quadratic curve fitting with no root, b) quadratic curve fitting with root 2, c) quadratic curve fitting with root 1 and d) the linear load-extension curve.

These three kinds of quadratic load-extension curves could be calculated in this work by adding the dotted blue curves to the blue curves in Figures 26a, 26b and 26c, to make the curves as complete parabolas.

It is thought that if the parameter m in Equation (69a) or in Equation (69b) is negative, the situation in Figure 26a is obtained. In this situation, no root is obtained when the load is equal to zero. This can occur because there are jamming forces in tight fabrics, and the red dotted curve in Figure 26a along with the blue curve is the actual load-extension curve which can be measured by a measuring tester.

When the parameter m is positive, the two cases are obtained as in Figures 26b and 26c. It is thought that two roots exist for Equations (73-76), namely root 1 and root 2, and slack fabrics in a dry relaxed state can be in root 1 or root 2 conditions, according to their relaxation from loaded knitting conditions. Fabrics in these conditions can be in a friction induced equilibrium state. If a relaxed fabric is in root 2 condition and the extension load is applied, load-extension rate results are obtained as in Figure 26b. Again, if a fabric is in root 1 condition and the extension load is applied, load-extension rate results are obtained as in Figure 26c. The red dotted line given in Figure 26c along with the blue line is the actual load-extension curve which can be obtained by using a measuring tester.

The negative m case, the root 1 case, and the root 2 case obtained during the present experimental work are given in Figures 12-15 for glass samples. Calculations of extension and contraction rates are also given in Equations (71, 85-88). Apart from these, example calculations of extension and contraction rates in relation to the tightness of fabrics are given in APPENDIX C for glass samples.

When Kurbak's work [11] is examined, it can be seen that root 1 and root 2 conditions also exist in plain knitted glass fabrics.

iii) In complex knitted fabrics, the other curve fittings obtained are the linear regression equation which is given in Figure 26d.

While linear regression equations were obtained for the wale-wise load-extension properties in plain knitted fabric because of the yarn arms of plain knitted fabrics which were nearly two dimensional, the linear regression equations obtained for three dimensional complex weft knitted fabrics are because of higher bending rigidities along with higher tightness. Linear regression equations are obtained in tight aramid fabrics. It is thought that these tight complex weft knitted fabrics with higher bending rigidities also have parabolic load-extension or load-contraction curves, but their extensions or contractions are too small to be approximated by linear curve fittings.

iv) As the initial regions of the load-extension and load-contraction properties of complex weft knitted fabrics are uncertain geometrically, some empirical equations are suggested for use in related engineering software. It is thought that, at least for experimentally considered tightness regions here, intermediate load-extension and load-contraction properties can be estimated. These empirical equations are given as in APPENDIX B.

v) In Empirical Equations given in APPENDIX B, the estimations of the Poisson's ratios of the structures are also given. They are listed below along with the Poisson's ratio obtained by Kurbak [11] for plain knitted glass fabrics as

$v = 0.5$	for plain knitted fabric
$v = 0.4288$	for 1x1 rib
$v = 0.3874$	for milano rib
$v = 0.1996$	for half cardigan
$v = 0.1930$	for full cardigan derivative

These estimations of Poisson's ratios are reasonable since they decrease according to the complexity of the structure, as they should be.

vi) According to the method given above, the experimentally obtained load-extension results for all the samples concerned here are compared with the given Empirical Equations in APPENDIX B in Figures 18-25 in which the extension or contraction rates are calculated with the similar equations as in Equations (71, 85-88). In most of the cases, the calculated load-extension curves fit with the experimentally obtained results.

More research, however, must be conducted by having more load levels in the region during experiments at any tightness point and also to increase the tightness points to cover intermediate tightness. It is thought that with this future research, the parameters c_0 , w_0 , and m in Table 6 can be formulated in relation to the tightness, l/d , and, thus, the above procedure will become a complete method.

Finally, some suggestions can be made on some of the technical applications of knitted fabrics according to the present results.

- If the load and extension rate relationship is uncertain as in Figures 26b and 26c, it cannot be used for cyclic loading, for example, for "stretch sensor" applications (see ref. [20]).

- In composite reinforcement application of knitted fabrics; Araujo et al. [21] suggested that if a fabric is extended at a certain rate, the low load region of the load-extension curves can be omitted and the breaking strengths of composites can be increased. They used this method with a 20% extension rate.

According to the present work, this suggestion is not suitable for every tightness of the fabric since the fixed amount of extension rate could be bigger than the maximum extension of tight fabrics. Apart from this, fabrics can be in one of the load-extension curves given in Figure 26; therefore, with a 20% extension (for example, if a fabric is in root 1 condition as in Figure 26c), the low tension region will not be completely omitted. It is thought that, instead of using a certain extension rate, the certain amount of load applied on a loop should be more suitable to use.

In addition to the above argument that the wale-wise breaking strengths of the composites reinforced with the plain knitted fabrics and the milano rib fabrics are obtained to be higher than the other weft knitted structures in practice, it is interesting to see that the wale-wise extensions of plain-knitted fabrics and the milano rib fabrics start from their relaxed conditions given in Figures 26a, 26b and 26d as seen in Figure 19a, Figure 23a, and Figure 6 of the reference paper by Kurbak [11].

- Lastly, the mechanical properties of fabrics are calculated by using their geometrical models nowadays (see refs. [22, 23]). Before starting of these kinds of calculations, the initial load-extension properties of the subjected fabric should first be experimentally investigated. Otherwise, some discrepancies may occur between the theoretically calculated values and the measured experimental results. There is one exception: if a fabric has a special tightness at which the course and/or wale jamming has just started to occur, on this special tightness point, the m value becomes zero. For this special tightness point, theoretical calculations can be carried out without the need for the initial experimental results.

6. CONCLUSION

In this work, an experimental investigation on the initial load-extension and load-contraction properties of some complex weft knitted technical fabrics was carried out based on the work of Kurbak [11] in plain knitted glass fabrics. The work is summarized and the conclusion given below:

- Two types of yarn were used namely 136 tex E-glass and 168 tex aramid. Four different structures were chosen: 1x1 rib, milano rib, half cardigan, and full cardigan derivative. Two types of samples were prepared for the wale-wise direction and the course-wise direction. For the 1x1 rib, three tightness points were taken: the 6 cam setting, the 8 cam setting, and the 10 cam setting of the 7 gauge V-bed hand knitting machine. For the milano rib, the half cardigan, and full cardigan derivative, two tightness points were taken, the 8 cam setting and the 10 cam setting. Six samples for each experiment were prepared. A total of 216 samples were prepared.

Samples were adjusted so that the usable length (h) and width (b) were about 20x10 cm² plus enough length to hold them by a load-extension measuring apparatus.

One sample for each experimental point was used to measure the initial dimensional properties of the fabric: the loop length (l), the course-per-cm (cpc), and wales-per-cm (wpc).

The load-extension and load-contraction properties of the 20x10 cm² samples were then measured on a special apparatus (see Figure 4) using 5 level dead weights. The load levels were increased from zero to the maximum load of the first region. For every load level, the lengths (h) and the middle widths (b_{min}) of the samples were measured. Five samples for each experimental point were measured, and their averages were calculated.

- Regression analyses were carried out on the relation between the loads (T) and lengths (h) and also between the loads (T) and widths (b_{min}). Mostly quadratic curve fittings with higher correlation coefficients were obtained between the load-extension and the load-contraction results except that, for some, tight aramid fabrics linear regression equations could be applied to the experimental results with higher correlation coefficients.
- For comparison purposes, the regression equations (Equations 6 and Table 5) are written in terms of the loop parameters c_{av} , c_{min} , w_{av} , w_{min} , T_c and T_w using Equations (21-22, 26-27).
- The last obtained equations were then turned into the forms of equations as given in Equations (28-31) according to the assumption made about the separating method of the frictional restrains and/or fabric jamming forces from quadratic curve fittings. In the form of Equations (28-31) the m values were considered as the frictional restrains or/and fabric jamming forces for the unit structures of fabrics.
- For the first stages of extensions and contractions, Kurbak [11] gave some equations as Equations (32-35) to replace c_{min} and w_{min} values with the c_{av} and w_{av} values by assuming that the side edges of the samples follow parabolic curves under loading conditions (see Figure 5a). Equations (32-35) are applied to all the c_{min} and w_{min} values in the regression equations, and they are turned into the forms given in Equations (36-39). The parameters of all the obtained regression equations in the form of Equations (36-39) are given in Table 6. It is seen in Table 6 that the m values are small enough to be considered as frictional restrains and/or fabric jamming forces. Therefore, the assumption made about the separating method of the m values from quadratic curve fittings is the reasonable one.
- When all the parabolic curve fittings were examined, three kinds of situations were distinguished:
 - When parameter m is negative (in this case, when external load T_w or T_c is equal to zero), the square root in Equations

(53-56) become imaginary; therefore, no root is obtained. This situation was primarily obtained for tight fabrics.

- ii) When parameter m is positive; there are two roots, root 1 and root 2. The fabric can be in each of the roots when the external load is equal to zero. These cases— the negative m case, the root 1 case, and the root 2 case— are also given in Table 6 as 0, 1, and 2 respectively. One more case is that when the linear regression equation is applied. For the linear equation case, a “dash”(-) is used in Table 6.
- g) The first region (initial region) is the most geometrically uncertain region of the load-extension and load-contraction curves; thus, if one wants to obtain the mechanical properties of knitted fabrics by using their geometrical models, this region may create some problems. Therefore, the attempt was made to find out if some empirical equations can be given for this region that can be used in related engineering software. The empirical equations are given as in APPENDIX B. While obtaining the empirical equations, Poisson's ratios of the structures were also estimated. The estimated Poisson's ratios are reasonable since they reduce with the complexities of the fabrics, as they should be.
- h) In Empirical Equations given in APPENDIX B, the parameters c_0 , w_0 , and m values are taken from Table 6. It is already known that the parameters c_0 and w_0 are related to the tightness l/d . It is attempted to obtain some relationship between the m parameters and the tightness l/d , as given in Figures 12-15. It was thought that, to obtain the exact relations between the parameter m and the tightness l/d , some more tightness points should be taken from each fabric structure during the experiments.
- i) Using Table 6 and the Empirical Equations in APPENDIX B, the load-extension rates and load-contraction rates are obtained through some equations which are similar to Equations (71, 85-88) for all the cases considered here. The results obtained were compared with the experimentally obtained extension and contraction rates as given in Figures 18-25.

Figures 18-25 show that the Empirical Equations in APPENDIX B correctly estimated the extension and contraction rates. Because only 5 load levels are taken for the first extension or contraction region in this work, for 7 points out of 70 points, however, the c_0 or w_0 values were obtained, which are different from the given points in Table 6. The new points are also written in brackets in Table 6.

Finally, it can be concluded that three different parabolic curve fittings of the load-extension and load-contraction rates were obtained as given schematically in Figures 26a, 26b and 26c. The linear curve fittings were also obtained for tighter aramid fabrics. The three kinds of curve fittings in Figures 26a, 26b and 26c could be calculated by Empirical Equation in APPENDIX B through some equations similar to Equations (71, 85-88); thus, this can be considered as a new method. It is thought that, when this method

is improved by future experiments, it will be useful for obtaining the load-extension or load-contraction properties of such a geometrically uncertain region, namely the initial load-extension or load-contraction region.

ACKNOWLEDGEMENT

Experimental section of this work was partly supported by TUBITAK (Scientific and Technological Research Council of Turkey) through the project No.1002/114M022. The authors would like to thank to TUBITAK for this support. The authors would like to thank Assoc. Prof. Dr. Tuba Alpyıldız for her contributions during carrying out the experimental section of the work. The authors would like to thank also Dr. Gonca Balcı Kılıç, Ph D Students; Mehmet Korkmaz and Berrak Buket Avcı, MSc Student Gökberg Devrim, BSc Student Mehmet Çağatay Balıkçı and MSc Arch. Darioush Bashiri for their contributions during preparation of this paper.

The research received no specific grant any funding agency in the public, commercial, or not -for- profit sectors.

REFERENCES

- Hepworth, B. (1978), *The biaxial load-extension behavior of a model of plain weft-knitting - Part I*, J Text Inst, 69, 101–107.
- MacRory, B. M., McCraith, R., & McNamara, A. B. (1975), *The biaxial load-extension properties of plain weft-knitted fabrics — a theoretical analysis*, Text Res J, 45, 746–760.
- MacRory, B. M., & McNamara, A. B. (1967), *Knitted fabrics subjected to biaxial stress - an experimental study*, Text Res J, 37, 908–911.
- Popper, P. (1966), *The theoretical behavior of a knitted fabric subjected to biaxial stresses*, Text Res J, 36, 148–157.
- Shanahan, W. J., & Postle, R. (1974), *A theoretical analysis of the tensile properties of plain-knitted fabrics. Part I: the load extension curve for fabric extension parallel to the courses*, J Text Inst, 65, 200–212.
- Hong, H., De Araujo, M. D., Fanguero, R., et al. (2002), *Theoretical analysis of load-extension properties of plain weft knits made from high performance yarns for composite reinforcement*, Text Res J, 72, 991–995.
- Shanahan, W. J., & Postle, R. (1974), *A theoretical analysis of the tensile properties of plain-knitted fabrics Part II: the initial load-extension behavior for fabric extension parallel to the wales*, J Text Inst, 65, 254–260.
- Kurbak, A. (2017), *Geometrical and mechanical modelings of dry relaxed slack plain-knitted fabrics for the benefit of technical textile applications Part I: A geometrical model*, Text Res J, 87(7), 838-852.
- Kurbak, A. (2017), *Geometrical and mechanical modelings of dry relaxed slack plain-knitted fabrics for the benefit of technical textile application Part II: Mechanical modelling induced by friction*, Text Res J, 87(7), 853-864.
- Kurbak, A. (2018), *Load-extension properties of glass plain knitted technical fabrics- Part I: Some additions to the extension of the*

circular ring problem to make it applicable for a knitted loop head curve, Text Res J, 88(6), 654-666.

11. Kurbak, A. (2018), *Load-extension properties of glass plain knitted technical fabrics – Part II: Extensions in the course-wise and wale-wise directions*, Text Res J, 88(6), 667-695.
12. Twaron, A. (2012), *Versatile high-performance fibres*, Twaron product brochure final 40-001.
13. Hearle, J. W. S., Grosberg, P., & Backer, S. (1969), *Structural Mechanics of Fibres, Yarn and Fabrics*. New York, Sidney, Toronto: Wiley-Interscience.
14. Lomow, S. M., & Verpoest, I. (2006), *Model of shear of woven fabric and parametric description of shear resistance of glass woven reinforcement*, Composite Science and Technology, 66, 919-933.
15. Kurbak, A. (2018), *Teknik ipliklerin eğilme rijitlikleri ile ilgili çalışmalar*, Tekstil ve Mühendis, 25(109), 61-65 (In Turkish).
16. Dönmez, S., & Kurbak, A. (2000), *Some investigations on tuck knitted fabrics*, Knitting Technology, 22(3), 12-14.
17. Kurbak, A., & Alpyıldız, T. (2009), *Geometrical models for cardigan structures Part II: Half cardigan*, Text Res J, 79(18), 1635-1648.
18. Elmalı, H. (2008), *Elastan iplik kullanımının kumaş özelliklerine etkileri*, MSc. Thesis, Dokuz Eylül Üniversitesi Fen Bilimleri Enstitüsü, Tekstil Mühendisliği Anabilim Dalı, İZMİR (In Turkish).
19. Öztürk, S. (2015), *Örme kumaşlarda yük-uzama davranışları üzerine bazı çalışmalar*. MSc. Thesis, Dokuz Eylül Üniversitesi Fen Bilimleri Enstitüsü, Tekstil Mühendisliği Anabilim Dalı, İZMİR (In Turkish).
20. Qureshi, W., Guo, L., Peterson, J., et al. (2011), *Knitted wearable stretch sensor for breathing monitoring application*, ambience, 9 Sweden: Boras.
21. De Araujo, M. D., Fangueiro, R., & Hong, H. (2003), *Modelling And Simulation of the Mechanical Behaviour of Weft-Knitted Fabrics For Technical Applications Part I: General Considerations And Experimental Analyses*, AUTEX Research Journal, (3), 111-123.
22. Vassiliadis, S. G., Kallivretaki, A. E., & Provatidis, C. G. (2007), *Mechanical simulation of the plain weft knitted fabrics*, International Journal of Clothing Science and Technology, 19(2), 109-130.
23. Abghary, M. J., Hasani, H., & Nedoushan, R. J. (2016), *Numerical simulating the tensile behaviour of 1x1 rib knitted fabrics using a novel geometrical model*, Fibres and Polymers, 17(5), 795-800.

APPENDIX A

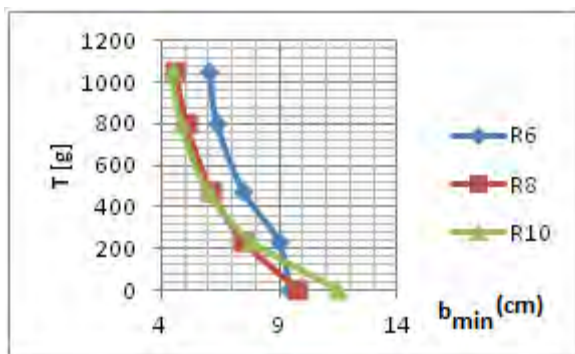
The experimentally obtained h and b_{min} values with changing load levels T are given in Tables A1a and A1b for wale-wise loaded glass samples, in Table A2a and A2b for course-wise loaded glass samples, in Table A3a and A3b for wale-wise loaded aramid samples and in Table A4a and A4b for course-wise loaded aramid samples.

Example drawings of load-extension and load contraction curves for each table are also given in Figures A1a, A1b, A2a, A2b, A3a, A3b A4a and A4b.

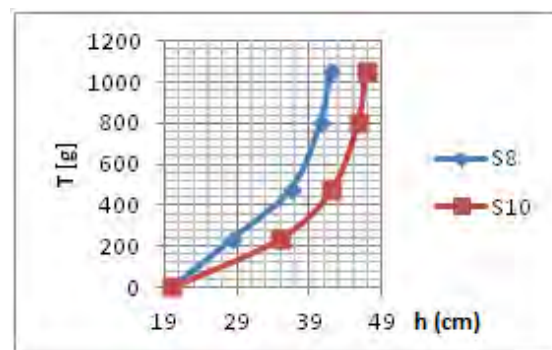
Table A1: Measured initial (the first stage) load-extension and load contraction results for wale-wise loaded glass samples.

Glass wale-wise extension Results									
a) extension (h) [cm]									
	1x1 Rib			Milano Rib		Half Cardigan		Full Cardigan Derivative	
Load [g]	R6	R8	R10	M8	M10	Y8	Y10	S8	S10
0	20	20	20	20	20	20	20	20	20
238.4	20.94	27.1	28.88	21.32	26.1	32.58	33.46	28.34	35.02
480	26.24	30.48	33	25.22	31.66	36.62	36.82	36.48	42.14
800	30.12	33.06	35.36	28.58	34.26	39.62	40.02	40.54	45.68
1050	30.92	33.92	36.24	29.88	35.48	40.9	40.98	41.98	46.8

b) contraction (b) [cm]									
	1x1 Rib			Milano Rib		Half Cardigan		Full Cardigan Derivative	
Load [g]	R6	R8	R10	M8	M10	Y8	Y10	S8	S10
0	9.5	9.8	11.5	8.7	11.5	10.8	11.7	11.5	14.2
238.4	9.0	7.5	7.8	8.3	9.2	9.2	9.5	9.9	10.7
480	7.4	6.1	6.0	7.0	6.7	8.5	8.7	8.4	8.3
800	6.3	5.0	4.8	5.8	5.5	7.8	8.2	7.2	6.8
1050	6.0	4.6	4.5	5.4	5.0	7.5	8.0	6.8	6.4



(a)



(b)

Figure A1: Example drawings of load-extension and load-contraction results given in Table A1; a) load-extension, b) load-contraction.

Table A2: Measured initial (the first stage) load-extension and load-contraction results for course-wise loaded glass samples.

Glass course-wise extension Results

a) extension (h) [cm]

	1x1 Rib			Milano Rib		Half Cardigan		Full Cardigan Derivative	
Load [g]	R6	R8	R10	M8	M10	Y8	Y10	S8	S10
0	20	20	20	20	20	20	20	20	20
238.4	23.22	40.82	57.26	22.04	25.66	39.3	50.2	40.04	45.52
480	30.72	49.86	66.26	24.9	30.08	46.6	56.1	46.66	49.08
800	38.48	55.58	70.32	28.3	33.26	51.34	60.34	51.74	52.08
1050	41.88	57.76	72.08	29.88	34.02	53	61.66	53.04	52.9

b) contraction (b) [cm]

	1x1 Rib			Milano Rib		Half Cardigan		Full Cardigan Derivative	
Load [g]	R6	R8	R10	M8	M10	Y8	Y10	S8	S10
0	10.1	6.7	8.6	9.2	9.7	9.3	9.0	8.3	8.6
238.4	9.7	4.5	3.6	8.8	7.8	8.1	6.8	7.3	6.2
480	8.6	3.1	2.4	7.7	5.5	7.2	5.8	6.5	5.2
800	6.6	2.5	2.0	6.0	3.8	6.4	5.1	5.7	4.3
1050	5.9	2.3	1.8	5.1	3.4	5.9	4.7	5.4	4.0

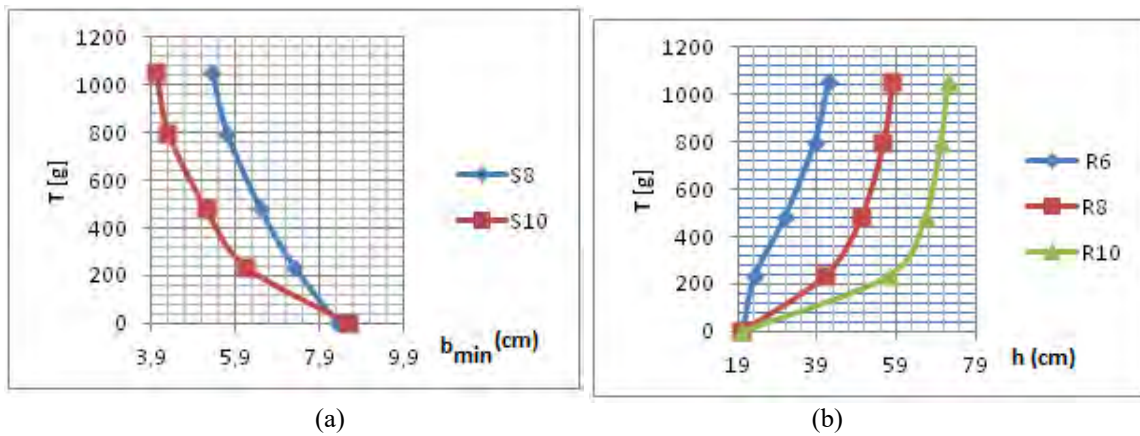
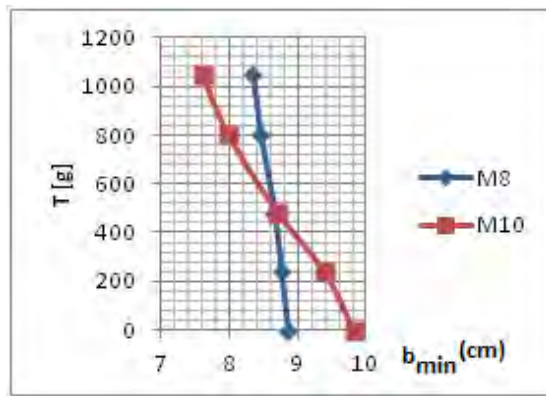


Figure A2: Example drawings of load-extension and load-contraction results given in Table A2; a) load-extension, b) load-contraction.

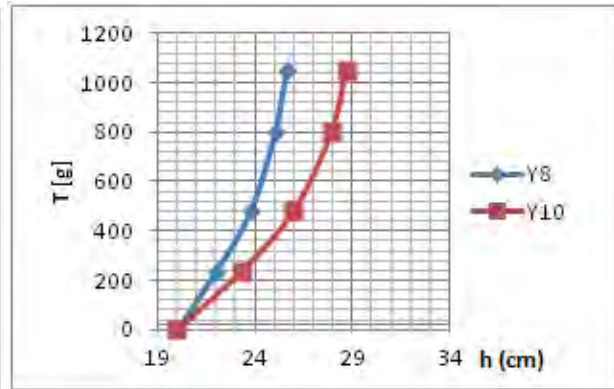
Table A3: Measured initial (the first stage) load-extension and load-contraction results for wale-wise loaded aramid samples.

Aramid wale-wise extension Results									
a) extension (h) [cm]									
	1x1 Rib			Milano Rib		Half Cardigan		Full Cardigan Derivative	
Load [g]	R6	R8	R10	M8	M10	Y8	Y10	S8	S10
0	20	20	20	20	20	20	20	20	20
238.4	20.36	20.42	24.96	20.12	21.26	22.02	23.28	21.64	25.4
480	20.62	22.76	33.06	20.46	23.36	23.78	25.98	24.6	27.92
800	21.1	25.72	36	21.08	25.44	25.04	27.92	27.2	29.52
1050	21.46	26.9	36.82	21.46	26.24	25.62	28.68	28.04	30.1

b) contraction (b) [cm]									
	1x1 Rib			Milano Rib		Half Cardigan		Full Cardigan Derivative	
Load [g]	R6	R8	R10	M8	M10	Y8	Y10	S8	S10
0	7.8	10.1	12.1	8.9	9.8	11.7	12.2	11.3	13.2
238.4	7.6	9.9	10.1	8.8	9.4	11.4	11.6	11.2	12.4
480	7.5	9.2	8.1	8.7	8.7	11.0	11.1	10.9	11.5
800	7.3	8.3	7.4	8.5	8.0	10.6	10.6	10.4	10.6
1050	7.2	7.9	7.2	8.3	7.6	10.5	10.4	10.1	10.2



(a)



(b)

Figure A3: Example drawings of load-extension and load-contraction results given in Table A3; a) load-extension, b) load-contraction.

Table A4: Measured initial (the first stage) load-extension and load-contraction results for course-wise loaded aramid samples.

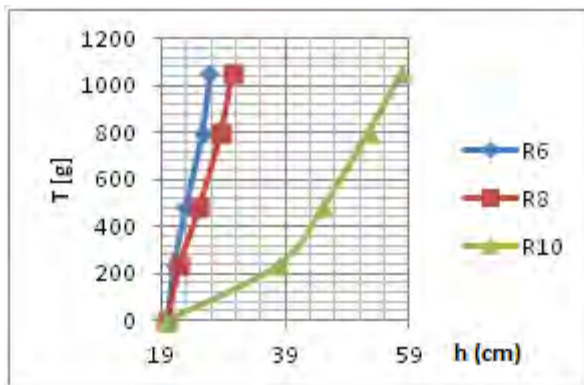
Aramid course-wise extension Results

a) extension (h) [cm]

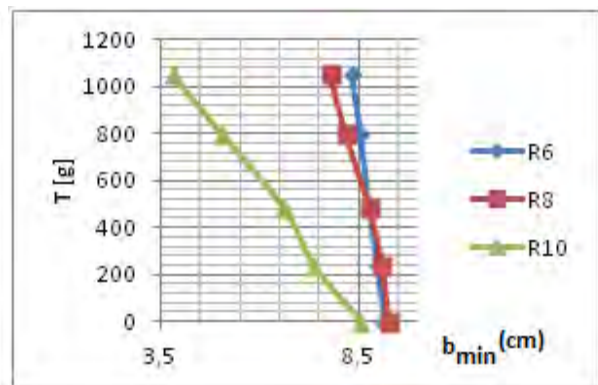
	1x1 Rib			Milano Rib		Half Cardigan		Full Cardigan Derivative	
Load [g]	R6	R8	R10	M8	M10	Y8	Y10	S8	S10
0	20	20	20	20	20	20	20	20	20
238.4	21.02	21.94	38.08	20.22	21.42	25.36	40.74	27.18	42.94
480	22.92	25.1	45.08	20.62	23.14	31.02	47.84	33.98	49.06
800	25.56	28.64	52.48	21.32	25.54	35.4	52.54	38.8	53
1050	26.8	30.5	57.76	21.78	27.08	37.16	54.2	40.52	55.04

b) contraction (b) [cm]

	1x1 Rib			Milano Rib		Half Cardigan		Full Cardigan Derivative	
Load [g]	R6	R8	R10	M8	M10	Y8	Y10	S8	S10
0	9.1	9.3	8.5	9.6	10.2	9.5	8.3	8.1	7.1
238.4	9.0	9.1	7.4	9.6	9.9	9.3	7.5	7.9	6.3
480	8.8	8.8	6.6	9.5	9.5	8.8	6.5	7.6	5.4
800	8.5	8.2	5.0	9.3	8.8	8.3	5.7	7.1	4.7
1050	8.3	7.8	3.8	9.1	8.4	8.0	5.3	6.8	4.3



(a)



(b)

Figure A4: Example drawings of load-extension and load-contraction results given in Table A4; a) load-extension, b) load-contraction.

APPENDIX B
EMPIRICAL EQUATIONS
A) GLASS
I) 1x1 RIB STRUCTURE
a) for wale-wise loaded samples
i) contraction

$$w_{av} = w_0 - v \frac{(w_0-d)^{1.3826} \sqrt{T_w/2+m/2}}{3.4231 \sqrt{B}} \quad (\text{B1})$$

ii) extension

$$c_{av} = c_0 + \frac{c_0 \sqrt{T_w/2+m/2}}{3.7080 \sqrt{B}} \quad (\text{B2})$$

b) for course-wise loaded samples
i) contraction

$$c_{av} = c_0 - v \frac{c_0^{n_1} \sqrt{T_c+m}}{3.7080 \sqrt{B}} \quad (\text{B3})$$

ii) extension

$$w_{av} = w_0 + \frac{(w_0-d)^{n_2} \sqrt{T_c+m}}{3.4231 \sqrt{B}} \quad (\text{B4})$$

where

$$v = \frac{1}{2.3319} = 0.4288 \quad (\text{B5})$$

$$n_1 = 2.6582 - 2.1194 (c_0/d - 3.7932) \quad (\text{B6})$$

$$n_2 = 2.34071 (w_0/d - 5.5671)^{-1/3.25} \quad (\text{B7})$$

A) GLASS
II) MILANO RIB STRUCTURE
a) for wale-wise loaded samples
i) contraction

$$w_{av} = w_0 - v \frac{(w_0-d)^{1.675} \sqrt{T_w/2+m/2}}{4.4476 \sqrt{B}} \quad (\text{B8})$$

ii) extension

$$c_{av} = c_0 + \frac{c_0^{2.163} \sqrt{T_w/2+m/2}}{4.9330 \sqrt{B}} \quad (\text{B9})$$

b) for course-wise loaded samples
i) contraction

$$c_{av} = c_0 - v \frac{c_0^{n_1} \sqrt{T_c+m}}{4.9330 \sqrt{B}} \quad (\text{B10})$$

ii) extension

$$w_{av} = w_0 + \frac{(w_0-d)^{n_2} \sqrt{T_c+m}}{4.4476 \sqrt{B}} \quad (\text{B11})$$

where Poisson's ratio

$$v = \frac{1}{2.5816} = 0.3874 \quad (\text{B12})$$

$$n_1 = 2.4441 - \frac{(c_0/d - 5.52)}{1.6674} \quad (\text{B13})$$

$$n_2 = 2.44034 - \frac{w_0/d - 5.8590}{3.7364} \quad (\text{B14})$$

A) GLASS
III) HALF CARDIGAN STRUCTURE
a) for wale-wise loaded samples
i) contraction

$$w_{av} = w_0 - v \frac{(w_0-d)^{n_1} a \sqrt{T_w/2+m/2}}{1.2504 \sqrt{B}} \quad (\text{B15})$$

ii) extension

$$c_{av} = c_0 + \frac{c_0^{0.65} \alpha \sqrt{T_w/2+m/2}}{3.5498\sqrt{B}} \quad (B16)$$

b) for course-wise loaded samples

i) contraction

$$c_{av} = c_0 - v \frac{c_0^{n_2} (1/\alpha) \sqrt{T_c+m}}{3.5498\sqrt{B}} \quad (B17)$$

ii) extension

$$w_{av} = w_0 + \frac{(w_0-d)^{n_3} (1/\alpha) \sqrt{T_c+m}}{1.2504\sqrt{B}} \quad (B18)$$

where Poisson's ratio and a constant, a , are as

$$v = \frac{1}{5.0094} = 0.1996 \quad (B19)$$

$$a = 1.2891 \quad (B20)$$

$$n_1 = 0.2506 - \frac{w_0/d - 9.1484}{23.4858} \quad (B21)$$

$$n_2 = 2.8312 - (c_0/d - 4.8031)/1.5423 \quad (B22)$$

$$n_3 = 0.7535 - (w_0/d - 12.2359)/32.4436 \quad (B23)$$

A) GLASS

IV) FULL CARDIGAN DERIVATIVE

a) for wale-wise loaded samples

i) contraction

$$w_{av} = w_0 - v \frac{(w_0-d)^{1.517} \alpha \sqrt{T_w/2+m/2}}{2.2267\sqrt{B}} \quad (B24)$$

ii) extension

$$c_{av} = c_0 + \frac{c_0^{n_1} a \sqrt{T_w/2+m/2}}{0.8065\sqrt{B}} \quad (B25)$$

b) for course-wise loaded samples

i) contraction

$$c_{av} = c_0 - v \frac{(1/\alpha) \sqrt{T_c+m}}{0.8065\sqrt{B}} \quad (B26)$$

ii) extension

$$w_{av} = w_0 + \frac{(w_0-d)^{n_2} (1/\alpha) \sqrt{T_c+m}}{2.2267\sqrt{B}} \quad (B27)$$

where

$$v = \frac{1}{5.1798} = 0.1930 \quad (B28)$$

$$a = 0.9762 \quad (B29)$$

$$n_1 = -0.037338 - \frac{c_0/d - 6.8443}{90.9019} \quad (B30)$$

$$n_2 = 0.7555 - \frac{(w_0/d - 12.6400)}{30.7872} \quad (B31)$$

B) ARAMID

I) 1x1 RIB STRUCTURE

a) for wale-wise loaded samples

i) contraction

$$\left. \begin{matrix} R6 \\ R8 \end{matrix} \right\} w_{av} = w_0 - v \frac{(w_0-d)^{n_1} a T_w}{0.5662(2B) 2} \quad (B32)$$

$$R10 \left. \right\} w_{av} = w_0 - v \frac{(w_0-d)^{n_1} a \sqrt{T_w/2+m/2}}{0.5662\sqrt{B}} \quad (B33)$$

ii) extension

$$\left. \begin{matrix} R6 \\ R8 \end{matrix} \right\} c_{av} = c_0 + \frac{c_0^{n_2} a T_w}{3.1709(2B) 2} \quad (B34)$$

$$R10\} c_{av} = c_0 + \frac{c_0^{n_2} a \sqrt{T_w/2+m/2}}{3.1709\sqrt{B}} \quad (B35)$$

b) for course-wise loaded samples

i) contraction

$$c_{av} = c_0 - v \frac{c_0^{n_3} (1/a)}{3.1709 (2B)} T_c \quad (B36)$$

ii) extension

$$\begin{matrix} R6\} \\ R8\} \end{matrix} w_{av} = w_0 + \frac{(w_0-d)^{n_4} (1/a)}{0.5662(2B)} T_c \quad (B37)$$

$$R10\} w_{av} = w_0 + \frac{(w_0-d)^{n_4} (1/a) \sqrt{T_c+m}}{0.5662\sqrt{B}} \quad (B38)$$

where Poisson's ratio

$$v = \frac{1}{2.3319} = 0.4288 \quad (B39)$$

$$a = 1.0500 \quad (B40)$$

$$n_1 = \begin{cases} -12.4049 + 2.2727 \frac{w_0}{d}; & \text{for } \frac{w_0}{d} \leq 5.6671 \\ 0.2520; & \text{for } \frac{w_0}{d} \geq 5.6671 \end{cases} \quad (B41)$$

$$n_2 = \begin{cases} -343.9483 + 137.3074 \frac{c_0}{d}; & \text{for } \frac{c_0}{d} \leq 2.5401 \\ 3.3608; & \text{for } \frac{c_0}{d} \geq 2.5401 \end{cases} \quad (B42)$$

$$n_3 = \begin{cases} 3.6553 + 25.3303(c_0/d - 2.5730); & \text{for } \frac{c_0}{d} \leq 2.5730 \\ 3.6553 + (c_0/d - 2.5730)/2.1812; & \text{for } \frac{c_0}{d} \geq 2.5730 \end{cases} \quad (B43)$$

$$n_4 = \begin{cases} -1.9575 + \frac{w_0}{1.9235}; & \text{for } \frac{w_0}{d} \leq 5.6671 \\ 1.2957; & \text{for } \frac{w_0}{d} \geq 5.6671 \end{cases} \quad (B44)$$

B) ARAMID

II) MILANO RIB STRUCTURE

a) for wale-wise loaded samples

i) contraction

$$w_{av} = w_0 - v \frac{(w_0-d)^{5.2548} (1/a) T_w}{34.6900(2B) \cdot 2} \quad (B45)$$

ii) extension

$$c_{av} = c_0 + \frac{c_0^{4.7778} (1/a) T_w}{8.3467 (2B) \cdot 2} \quad (B46)$$

b) for course-wise loaded samples

i) contraction

$$c_{av} = c_0 - v \frac{c_0^{3.6933} a}{8.3467 (2B)} T_c \quad (B47)$$

ii) extension

$$w_{av} = w_0 + \frac{(w_0-d)^{4.5893} a}{34.6900(2B)} T_c \quad (B48)$$

where

$$v = \frac{1}{2.5949} = 0.3857 \quad (B49)$$

$$a = 1.2369 \quad (B50)$$

B) ARAMID

III) HALF CARDIGAN STRUCTURE

a) for wale-wise loaded samples

i) contraction

$$w_{av} = w_0 - v \frac{(w_0-d)^{n_1} \sqrt{T_w/2+m/2}}{0.5016\sqrt{B}} \quad (B51)$$

ii) extension

$$c_{av} = c_0 + \frac{c_0^{n_2} \sqrt{T_w/2+m/2}}{0.7295\sqrt{B}} \quad (B52)$$

b) for course-wise loaded samples

i) contraction

$$\left. \begin{array}{l} Y8 \\ Y10 \end{array} \right\} c_{av} = c_0 - v \frac{c_0^{n_3}}{0.7295 (2B)} T_c \quad (B53)$$

$$Y10 \left. \right\} c_{av} = c_0 - v \frac{c_0^{0.8457} \sqrt{T_c+m}}{0.7295 \sqrt{B}} \quad (B54)$$

ii) extension

$$w_{av} = w_0 + \frac{(w_0-d)^{n_4} \sqrt{T_c+m}}{0.5016 \sqrt{B}} \quad (B55)$$

where

$$v = \frac{1}{5.0094} = 0.1996 \quad (B56)$$

$$n_1 = 0.1514 - 2.4037 (w_0/d - 7.07861) \quad (B57)$$

$$n_2 = -1.0356 + \frac{c_0/d - 3.5470}{1.616} \quad (B58)$$

$$n_3 = -0.2381 + \frac{c_0/d}{4.7227} \quad (B59)$$

$$n_4 = 0.7911 - \frac{w_0/d - 5.0750}{9.9688} \quad (B60)$$

B) ARAMID
IV) FULL CARDIGAN DERIVATIVE
a) for wale-wise loaded samples

i) contraction

$$\left. \begin{array}{l} S8 \\ S10 \end{array} \right\} w_{av} = w_0 - v \frac{(w_0-d)^{n_1} T_w}{0.7275 (2B) 2} \quad (B61)$$

$$S10 \left. \right\} w_{av} = w_0 - v \frac{(w_0-d)^{1.0142} \sqrt{T_w/2+m/2}}{0.7275 \sqrt{B}} \quad (B62)$$

ii) extension

$$c_{av} = c_0 + \frac{c_0^{n_2} \sqrt{T_w/2+m/2}}{0.7692 \sqrt{B}} \quad (B63)$$

b) for course-wise loaded samples

i) contraction

$$\left. \begin{array}{l} S8 \\ S10 \end{array} \right\} c_{av} = c_0 - v \frac{c_0^{n_3}}{0.7692 (2B)} T_c \quad (B64)$$

$$S10 \left. \right\} c_{av} = c_0 - v \frac{c_0^{0.8903} \sqrt{T_c+m}}{0.7692 \sqrt{B}} \quad (B65)$$

ii) extension

$$w_{av} = w_0 + \frac{(w_0-d)^{n_4} \sqrt{T_c+m}}{0.7275 \sqrt{B}} \quad (B66)$$

where

$$v = \frac{1}{5.1798} = 0.1930 \quad (B67)$$

$$n_1 = -3.2302 + \frac{w_0/d}{1.6392} \quad (B68)$$

$$n_2 = 7.2022 - 1.2190 c_0/d \quad (B69)$$

$$n_3 = 0.4086 + \frac{c_0/d}{8.7654} \quad (B70)$$

$$n_4 = 0.7410 - \frac{w_0/d - 9.5493}{7.7947} \quad (B71)$$

APPENDIX C
EXAMPLE CALCULATIONS OF THE PARAMETER m , THE RATES OF EXTENSIONS (ε_{1w} , ε_{1c}), AND THE RATES OF CONTRACTIONS (ε_{2w} , ε_{2c}) FOR GLASS SAMPLES

The following route and notations should be known in order to understand the calculations:

- i) c_0 and w_0 values should be taken from Table 6 for related cases
- ii) The linear relations between tightness points l/d and the parameter m of each fabric structure are assumed to occur as in Figures 12-15.
- iii) In the equations in the Appendix, notations as in Equations (77-84) are used. Evaluations of the right-hand side of Equations (77-84), in turn, should be made by using the related case equations given in Empirical Equations at APPENDIX B.

Example calculations are given below.

A) GLASS
1) 1x1 RIB STRUCTURE
a) Wale-wise loaded samples
i) Contraction

$$m = \begin{cases} -T_0 = 1.452 (l/d - 20.5); \text{ for } l/d \leq 20.5; m < 0 \\ \frac{(l/d - 20.5)}{12.8143}; \text{ for } l/d \geq 20.5; \text{ root } 2 \end{cases} \quad (C1)$$

$$\varepsilon_{2w} = \begin{cases} \frac{-D_{2w}(T_w/2 - T_0/2)}{w_0}; \text{ for } l/d \leq 20.5; T_w/2 \geq T_0/2 \\ \frac{-D_{2w}(m/2) - D_{2w}(T_w/2 + m/2)}{w_0 + D_{2w}(m/2)}; \text{ for } l/d \geq 20.5 \end{cases} \quad (C2)$$

ii) Extension

$$m = \begin{cases} -T_0 = 1.452 (l/d - 20.5); \text{ for } l/d \leq 20.5; m < 0 \\ \frac{(l/d - 20.5)}{6.3747}; \text{ for } l/d \geq 20.5; \text{ root } 1 \end{cases} \quad (C3)$$

$$\varepsilon_{1w} = \begin{cases} \frac{D_{1w}(T_w/2 - T_0/2)}{c_0}; \text{ for } l/d \leq 20.5; T_w/2 \geq T_0/2 \\ \frac{D_{1w}(m/2) + D_{1w}(T_w/2 + m/2)}{c_0 - D_{1w}(m/2)}; \text{ for } l/d \geq 20.5 \end{cases} \quad (C4)$$

b) Course-wise loaded samples
i) Contraction

$$m = \begin{cases} \frac{-(l/d - 20.5)}{1.6726}; \text{ for } l/d \leq 20.5; \text{ root } 1 \\ 1.122 (l/d - 20.5); \text{ for } l/d \geq 20.5; \text{ root } 2 \end{cases} \quad (C5)$$

$$\varepsilon_{2c} = \begin{cases} \frac{D_{2c}(m) - D_{2c}(T_c + m)}{c_0 - D_{2c}(m)}; \text{ for } l/d \leq 20.5 \\ \frac{-D_{2c}(m) - D_{2c}(T_c + m)}{c_0 + D_{2c}(m)}; \text{ for } l/d \geq 20.5 \end{cases} \quad (C6)$$

ii) Extension

$$m = \begin{cases} -T_0 = \frac{(l/d - 20.5)}{3.2389}; \text{ for } l/d \leq 20.5; m < 0 \\ \frac{(l/d - 20.5)}{1.067}; \text{ for } l/d \geq 20.5; \text{ root } 1 \end{cases} \quad (C7)$$

$$\varepsilon_{1c} = \begin{cases} \frac{D_{1c}(T_c - T_0)}{w_0}; \text{ for } l/d \leq 20.5; T_c \geq T_0 \\ \frac{D_{1c}(m) + D_{1c}(T_c + m)}{w_0 - D_{1c}(m)}; \text{ for } l/d \geq 20.5 \end{cases} \quad (C8)$$

II) MILANO RIB

a) Wale-wise loaded samples

i) Contraction

$$m = -T_0 = 1.3336 (l/d - 21.1425); \text{ for } l/d \leq 21.1425; m < 0 \quad (\text{C9})$$

$$\varepsilon_{2w} = -\frac{D_{2w}(T_w/2 - T_0/2)}{w_0}; \text{ for } l/d \leq 21.1425; T_w/2 \geq T_0/2 \quad (\text{C10})$$

ii) Extension

$$m = -T_0 = 1.3336 (l/d - 21.1425); \text{ for } l/d \leq 21.1425; m < 0 \quad (\text{C11})$$

$$\varepsilon_{1w} = \frac{D_{1w}(T_w/2 - T_0/2)}{c_0}; \text{ for } l/d \leq 21.1425; T_w/2 \geq T_0/2 \quad (\text{C12})$$

b) Course-wise loaded samples

i) Contraction

$$m = -1.3654 (l/d - 21.1425); \text{ for } l/d \leq 21.1425; \text{ root 1} \quad (\text{C13})$$

$$\varepsilon_{2c} = \frac{D_{2c}(m) - D_{2c}(T_c + m)}{c_0 - D_{2c}(m)}; \text{ for } l/d \leq 21.1425 \quad (\text{C14})$$

ii) Extension

$$m = -T_0 = \frac{(l/d - 21.1425)}{6.159}; \text{ for } l/d \leq 21.1425; m < 0 \quad (\text{C15})$$

$$\varepsilon_{1c} = D_{1c}(T_c - T_0)/w_0; \text{ for } l/d \leq 21.1425; T_c \geq T_0 \quad (\text{C16})$$

III) HALF CARDIGAN

a) Wale-wise loaded samples

i) Contraction

$$m = \frac{(l/d - 20.58)}{2.316}; \text{ for } l/d \geq 20.58; \text{ root 2} \quad (\text{C17})$$

$$\varepsilon_{2w} = \frac{-D_{2w}(m/2) - D_{2w}(T_w/2 + m/2)}{w_0 + D_{2w}(m/2)}; \text{ for } l/d \geq 20.58 \quad (\text{C18})$$

ii) Extension

$$m = \frac{(l/d - 11.8)}{4.5224}; \text{ for } l/d \geq 11.8; \text{ root 1} \quad (\text{C19})$$

$$\varepsilon_{1w} = \frac{D_{1w}(m/2) + D_{1w}(T_w/2 + m/2)}{c_0 - D_{1w}(m/2)}; \text{ for } l/d \geq 11.8 \quad (\text{C20})$$

b) Course-wise loaded samples

i) Contraction

$$m = \begin{cases} \frac{-(l/d - 22.75)}{2.284}; & \text{for } l/d \leq 22.75; \text{ root 1} \\ \frac{(l/d - 22.75)}{6.5624}; & \text{for } l/d \geq 22.75; \text{ root 2} \end{cases} \quad (\text{C21})$$

$$\varepsilon_{2c} = \begin{cases} \frac{D_{2c}(m) - D_{2c}(T_c + m)}{c_0 - D_{2c}(m)}; & \text{for } l/d \leq 22.75 \\ \frac{-D_{2c}(m) - D_{2c}(T_c + m)}{c_0 + D_{2c}(m)}; & \text{for } l/d \geq 22.75 \end{cases} \quad (\text{C22})$$

ii) Extension

$$m = \frac{(l/d - 20)}{1.0661}; \text{ for } l/d \geq 20; \text{ root 1} \quad (\text{C23})$$

$$\varepsilon_{1c} = \frac{D_{1c}(m) + D_{1c}(T_c + m)}{w_0 - D_{1c}(m)}; \text{ for } l/d \geq 20 \quad (\text{C24})$$

IV) FULL CARDIGAN DERIVATIVE

a) Wale-wise loaded samples

i) Contraction

$$m = \begin{cases} \frac{-(l/d-22.75)}{3.2863}; \text{ for } l/d \leq 22.75; \text{ root 1} \\ -T_0 = \frac{-(l/d-22.75)}{6.5095}; \text{ for } l/d \geq 22.75; m < 0 \end{cases} \quad (C25)$$

$$\varepsilon_{2w} = \begin{cases} \frac{D_{2w}(m/2) - D_{2w}(T_w/2 + m/2)}{w_0 - D_{2w}(m/2)}; \text{ for } l/d \leq 22.75 \\ \frac{-D_{2w}(T_w/2 - T_0/2)}{w_0}; \text{ for } l/d \geq 22.75; T_w/2 \geq T_0/2 \end{cases} \quad (C26)$$

ii) Extension

$$m = \begin{cases} -T_0 = \frac{(l/d-22.75)}{2.1654}; \text{ for } l/d \leq 22.75; m < 0 \\ \frac{(l/d-22.75)}{1.8837}; \text{ for } l/d \geq 22.75; \text{ root 1} \end{cases} \quad (C27)$$

$$\varepsilon_{1w} = \begin{cases} \frac{D_{1w}(T_w/2 - T_0/2)}{c_0}; \text{ for } l/d \leq 22.75; T_w/2 \geq T_0/2 \\ \frac{D_{1w}(m/2) + D_{1w}(T_w/2 + m/2)}{c_0 - D_{1w}(m/2)}; \text{ for } l/d \geq 22.75 \end{cases} \quad (C28)$$

b) Course-wise loaded samples

i) Contraction

$$m = \begin{cases} \frac{-(l/d-22.75)}{1.1680}; \text{ for } l/d \leq 22.75; \text{ root 1} \\ \frac{(l/d-22.75)}{5.9700}; \text{ for } l/d \geq 22.75; \text{ root 2} \end{cases} \quad (C29)$$

$$\varepsilon_{2c} = \begin{cases} \frac{D_{2c}(m) - D_{2c}(T_c + m)}{c_0 - D_{2c}(m)}; \text{ for } l/d \leq 22.75 \\ \frac{-D_{2c}(m) - D_{2c}(T_c + m)}{c_0 + D_{2c}(m)}; \text{ for } l/d \geq 22.75 \end{cases} \quad (C30)$$

ii) Extension

$$m = 2.2125 (l/d - 20); \text{ for } l/d \geq 20; \text{ root 1} \quad (C31)$$

$$\varepsilon_{1c} = \frac{D_{1c}(m) + D_{1c}(T_c + m)}{w_0 - D_{1c}(m)}; \text{ for } l/d \geq 20 \quad (C32)$$